Ludwig-Maximilians-Universität München

Non-Newtonian effects in silicate liquids and crystal bearing melts: Implication for magma dynamics

Dissertation
zur Erlangung des Doktorgrades
der Fakultät für Geowissenschaften der
Ludwig-Maximilians-Universität München

vorgelegt von
Benoît Cordonnier

am
2. März 2009

Datum der muendlichen Pruefung:

29. Juli 2009

1. Gutachter: Prof. Dr. Donald Bruce Dingwell

2. Gutachter: Prof. Dr. Hans-Peter Bunge

Tag der mündlichen Prüfung:

Contents

Summary

"The most beautiful we can experience is the mysterious. It is the source of all true art and science."

Albert Einstein

High-silica volcanic systems are considered to be the most devastating. Their highly viscous properties create a high pressurised non-fluent system which consequently relaxes the stress mostly by exploding through the brittle regime. Even if an explosion is avoided and the magma flows, it often generates lava domes at the top of the volcano; which, patiently, accumulate magmas that will rush down the slopes once the yield stress is crossed. Thus, such volcanoes have an explosive nature and often generate catastrophic pyroclastic flows.

The modelling of magma ascent inside eruptive conduits is commonly based on fluid mechanic principles. The difficulty of the approach is however not as much driven by the physical equations of the numerical model as the variability of the parameters of the magma itself. It is well established that the rheology of magma strongly depends on the temperature, the stress, the strain, the chemical composition, the crystal and the bubble contents. In other words, magmatic modelling involves a set of movement equations which call for a comportmental/rheological law. The movement equations give roughly equivalent results through the different models; however magma rheology is poorly controlled. The deformation of highly crystallised dome lavas is key to understanding their rheology and to fixing their failure onset. It is thus essential to adequately understand magma rheology before performing complex numerical models.

Here we focus on the well studied Unzen volcano, in Japan, which had a recent period of activity between 1990 and 1995. The dome building eruptions in Unzen generate repeated dome failure and pyroclastic flows. They vary in character and behaviour from effusive domes to brittle pyroclastic events. Since then, the Unzen Scientific Drilling Project, initiated in April 1999, drilled through the volcano and sampled the eruptive conduit. This provides us with rare original samples for study and characterisation. The physico-chemical properties of these valuable samples were determined with an array of devices. Of these a large uniaxial deformation press, which can operate at high load (0 up to 300KN), and temperature (25-1200°C), will be of utmost importance. This press deforms the samples under known parameters and allows us to determine the viscosity of the melt.

In this study we investigate the stress and strain-rate dependence on several glasses and Mt Unzen dome lavas. Their rheology has been determined for temperatures from 900 to 1010°C and stresses from 2 to 120 Mpa (60 MPa for crystal bearing melt) in uniaxial compression . This survey aims to distinguish the Non-Newtonian effects perturbing magmatic melts, also known as indicators of the brittle field. Towards our experiments we observed three majors viscosity decrease types: Two were dependant and typical of the solid fraction (Shear thinning & Time weakening effect). The first is instantaneous and on the whole recovered during stress release. The second is time dependent and non-recoverable. The third and last effect observed is attributed to the melt fraction and its self heating under stress (Viscous Heating Effect).

We extensively investigated this last effect on pure silicate liquids and crystal bearing melts. Our findings suggest that most of the Non-Newtonians effects observed in silicate melts are linked to a self heating of the sample and can subsequently be corrected with the temperature without involving other laws than a pure viscous material. Moreover we observed that this self heating reorganise the energy distribution within the sample and by localising the strain may favours the formation of shear banding and the apparition of 'hot cracks'.

Crystal bearing melts exhibit two more Non-Newtonian effects. The first one, the shear thinning, is typical of that observed in previous experiments on crystal-bearing melts. On crystal free melts, this viscosity decrease is observed at much lower magnitude. We infer that the crystal phase responds elastically to the stress applied and relaxes once the load is withdrawn. The second one, the time weakening effect, appears more complex and this regime depends on the stress (and/or strain-rate) history. We distinguish four different domains: Newtonian, non-Newtonian, crack propagation and failure domains. Each of these domains expresses itself as a different regime of viscosity decrease. Due to stress localisation, cracking appears in crystal-bearing melts (intra-phenocryst and/or the in the melt matrix) earlier than in crystal-free melts. For low stresses, the apparent viscosity is higher for crystal-bearing melts (as predicted by Einstein-Roscoe equations). However, while the stress (or strain rate) increases, the apparent viscosity is decreasing to that of the crystal-free melt and could be even lower if viscous heating effects are involved.

Consequently, we emphasise that any numerical simulation performed without taking into account the strain-rate dependencies described above would overestimate the apparent viscosity by orders of magnitude. The magma dynamics will appears slower than in reality. Exaggerating the viscosity of a volcanic dynamic system would overestimate the time range available for a potential evacuation of the red zones. Applying a more realistic rheology would improve the early warning tools and improve the safety of the population surrounding volcanic systems.

List of Figures

List of Tables

Acknowledgments

The " special acknowledgement of the week" goes for Bernhard Schuberth & Christina Plattner who are finishing roughly at the same time. I thank Tinie for her help through the bureaucracy of the submission and 'Bernard' for sharing his LaTeX template that saved me so much time.

Finally thank you to all the persons of this institute, I will not personally cite each of you to not forget any; but I guess that you all know why I am grateful today: For all this good time.

The following is my personal section:

Sssaanks to THE Muppet and Fabio for cheering me up during the 'black hole' of this survey where I was about to quit science.

Thank you to the White stripes, Vampire Week-end, Death cab for a cutie , Renaud, les laidgums without who this work would have never end. ....

I dedicate this work to my friends and 'brothers' from Bretagne and to the "néoténiques" . But it goes first to my parents who had the unfaithful destiny to have two scientists as sons. At least one of them is brilliant: "Bisous Titom, continues de révolutionner la Biologie cellulaire ... Maman, t'as pas finie d'en baver". A mon pre et ma mre: "Merci, d'avoir été les premiers à m apprendre; en particulier le plus important".

Introduction

Initially this survey aimed to characterise Mt. Unzen volcano rheology and produce a numerical code reflecting the 1990-1995 eruption. Only half of our objectives have been completed. It was not so much the difficulty of producing a working code that brought us to redefine the subject, but more the desire to fully understand the rheology of volcanic melts.

During experimental measurements of Mt.Unzen volcano, it became apparent that its rheology was non-linear and is affected by many processes. At this stage of the work, I felt it was more exciting to understand and constrain the comportmental law ruling Mt.Unzen rheology rather than defining a numerical code based on a approximate behaviour. Indeed, Navier-Stokes equation set is quite well defined, based on Newton principles and continuum mechanics. Moreover, coding a numerical simulation of a cylindrical volcanic conduit would not have brought so much as excellent models on the problem already exist [*Massol and Jaupart* 1999; *Melnik and Sparks* 1999; *Massol et al.* 2001; *Massol and Koyaguchi* 2005; *Melnik et al.* 2005; *Costa et al.* 2007]. On the contrary, some black holes remain in rheophysics where the limits are still not clearly defined. Consequently it appeared more important to improve our knowledge of the 'fuel' of numerical simulations: the fluid comportmental law.

In terms of silicate melt rheology, the Ludwig Maximilians Universität is one of the leading institutions worldwide. Its facilities, connections and more globally,

its knowledge on the subject, provide a unique opportunity to carry out such investigations. However, before investigating Mt. Unzen rocks in more details, we needed to better constrain the effects driving the rheology of pure silicate liquids. Before elaborating models on complex multi-phase magmas (liquids-crystals-bubbles); we had to differentiate what was the non-Newtonian rheology of a simple system.

Accordingly, by investigating a well known homogeneous standard glass we aimed to control and understand stress and strain-rate distribution within our sample and its impact on the dynamic. This first estimation brought us to consider the energy balance affecting our sample. While doing this we faced the already known strain-rate dependent viscosity of silicate melts. Dr. K.-U. Hess was, at this time, curious about the importance of the viscous heating effect. Inserting a thermocouple within the sample offered a first positive test of the importance of viscous heating.

After the successful standard glass experiments we returned to the natural Unzen samples. We affronted unexpected effects such as the instantaneous decrease of the apparent viscosity. Going back and force between pure liquids and crystal bearing melts we ensured the effects observed and their potential sources.

Two conclusions comes out of this survey. The viscous heating effect can explain most of the non-Newtonian behaviour measured. Crystals act in a elasto-brittle way and reduce significantly the apparent viscosity.

It is hoped these results will lead to a generalised brittle theory but at least improve our knowledge of magma dynamics.

Note: we decided to not present the details of the press calibration, software developed for the analysis of the data, numerical finite element code(s) or to review the history of the 1990-1995 eruption of Mt.Unzen. However, all of this work has been discussed in previous posters and talks. If the committee finds it relevant to add any of those details in the final version of this manuscript, we would be pleased to implement these changes in the relevant appendices.

Chapter 1

Viscous heating and the rheology of crystal free melts: experimental investigation

"Science has proof without any certainty. Creationists have certainty without any proof."

Ashley Montagne

This chapter treats of the experiments conducted to trigger the viscous heating effect on a natural Icelandic rhyolitic glass. Viscous heating during magmatic flow may play a major role in eruption dynamics. In order to document viscous heating during deformation of magma, we have conducted a series of deformation experiments where viscous heating is directly monitored via thermocouples in high-viscosity magmas. We observe experimentally the strain-rate dependence of viscous heating. Viscous heating becomes rheologically significant in the highly viscous lavas investigated at strain rates above ca. 10^{-3} s^{-1}. A simple analysis shows that the temperature increase generated through viscous heating during deformation of melts with viscosities ranging from 108 to 1012 Pas can account for their apparent non-Newtonian rheology in these experiments. This thermal correction transforms apparent non-Newtonian, strain-rate dependent rheology of magma to a Newtonian behavior over the range of conditions accessed in this work. In this manner, this study provides an experimental basis for separating the relative roles of structural relaxation and viscous heating in the generation of apparent non-Newtonian rheology at high strain rates. Here, viscous heating dominates and the observation of the structural onset of non-Newtonian behavior is precluded by a viscous-heating-induced lowering of the Newtonian viscosity. The interplay of viscous heating and structural relaxation in melts in nature is discussed briefly.

1.1   Introduction

One of the most remarkable, unpredictable and (from the point of view of monitoring) alarming aspects of explosive volcanic centers is their ability to switch from low-risk effusive to high-risk explosive eruptive behavior. A physical un-

derstanding the ductile-brittle transition is an essential aspect of distinguishing criteria for the choice such a system makes between effusive and explosive eruptions. It is likely that competition between the strain rate and the structural relaxation timescale of a melt ultimately dictates whether the eruption will remain effusive or explode [*Dingwell* 1996]. The structural relaxation timescale (t) is defined by Maxwell as:

$$\tau = \frac{\eta_s}{G_\infty} \tag{1.1}$$

where η_s is the shear viscosity and G_∞ the infinite frequency elastic shear moduli (approximated at 10^{10} +/- 0.5 Pa for silicate melts [*Dingwell and Webb* 1989]). High-temperature macroscopic rheological experiments have demonstrated that this transition, that of a Newtonian fluid to a non-Newtonian, strain-rate dependent fluid rheology, can occur at a strain rate approximately one 1000th that of the structural relaxation timescale [*Webb and Dingwell* 1990a]. For high-viscosity silicate melts (e.g., 10^{10} Pas), this would translate to an onset at 10^{-3} s^{-1}. Silicate magmas flowing under such conditions are however, also expected to generate significant temperature increase through the viscous heating which the deformation generates in them [*Rosi et al.* 2004; *Tuffen and Dingwell* 2005]. The strong temperature-dependence of Newtonian viscosity means that if significant viscous heating can occur then it will likely have rheological consequences for the magma [*Shaw* 1969; *White and Muller* 2000a]. Viscous energy dissipation (also termed viscous heating, viscous dissipation, and shear heating) is the contribution to the total energy made by irreversible deformational work [*Holtzman et al.* 2005]. In magmatic and volcanic systems, viscous heating is commonly inferred in shear

zones [*Holtzman et al.* 2005], dikes [*Carrigan et al.* 1992], along the conduit margins [*Boyd* 1961; *Fujii and Uyeda* 1974; *Hardee and Larson* 1977; *Fujita et al.* 2000; *Mastin* 2002; *Polacci et al.* 2004; *Rosi et al.* 2004; *Mastin* 2005a; *Vedeneeva et al.* 2005; *Hale and Muhlhaus* 2007], in lava domes [*Smellie et al.* 1998], and in low-viscosity lava flows [*Dragoni et al.* 2002; *Keszthelyi* 1995a; *Pearson* 1977]. Recent numerical modelling of viscous heating in a conduit has demonstrated the strong influence of viscous heating along the conduit margin and, as a result, the importance of considering plug-like ascent profiles instead of Poiseuille flows [*Costa and Macedonio* 2003a; *Mastin* 2005a]. Here we report results from a series of uniaxial compression experiments on natural and synthetic silicate melts that have been performed in order to characterize in situ the heat generated by viscous dissipation during increasing strain rates. The viscosity-temperature dependence of the two selected melts (i.e., depolymerized NIST 717a vs polymerized rhyolitic obsidian from Iceland) encompasses the variations given by natural melts [*Mysen* 1987]. Here, correction of apparent non-Newtonian rheology for the thermal influence of viscous heating reveals a rheology which is independent of strain rate within experimental error.

1.2   Method

The present viscosity measurements were made with a unique high-load, high-temperature uniaxial press [*Hess et al.* 2007] capable of ascerting viscosity within a precision of +/- 0.06 log Pa*s. In order to adequately quantify viscous heating effects in rheologically simple silicate melts, we have performed measurements on NIST reference standard silicate glass SRM 717a (a standard silicate glass used to check test methods and calibrate equipment for the determination of the

Table 1. Chemical compositions of samples.

	NIST 717a	Obsidian
SiO_2	68	74.0
Al_2O_3	3.5	12.9
Na_2O	1	5.2
K_2O	8	3.6
CaO	0	1.0
MnO	0	0.1
MgO	0	0.2
Fe_2O_3	0	0.7
FeO	0	1.7
TiO_2	0	0.2
Li_2O	1	nd
B_2O_3	18.5	nd
water	0	0.3
total	100	100.0

Table 1.1: Chemical compositions of samples investigated.

viscosity of glass in accordance with ASTM Procedure C 965-81) for which the temperature-dependence of viscosity is well-known [*Hess et al.* 2007] and on calc-alkaline rhyolitic obsidian for which we have measured the temperature-dependent Newtonian viscosity (Table 1.2). The NIST viscosity standard was chosen as an essential prerequisite for studies on natural rhyolite due to its extremely well characterised rheology and homogeneity.

Cylindrical samples with a height of 40 mm and a diameter of 20 mm were prepared by cutting, drilling and grinding. Three holes of 2-mm diameter, equally spaced along the samples axis, were radially drilled through to the centre in order to insert three thermocouples for precise monitoring of temperature variation during the experiments (Figure 1.2). For this study we used shielded (Inconel) NiCr-Ni thermocouples (T.M.H., Hanau, Germany, Type K, D=1.5 mm) with a precision of +/- 0.5 K and a thermal response of approximately 1 s to attain 63 % of the exact temperature.
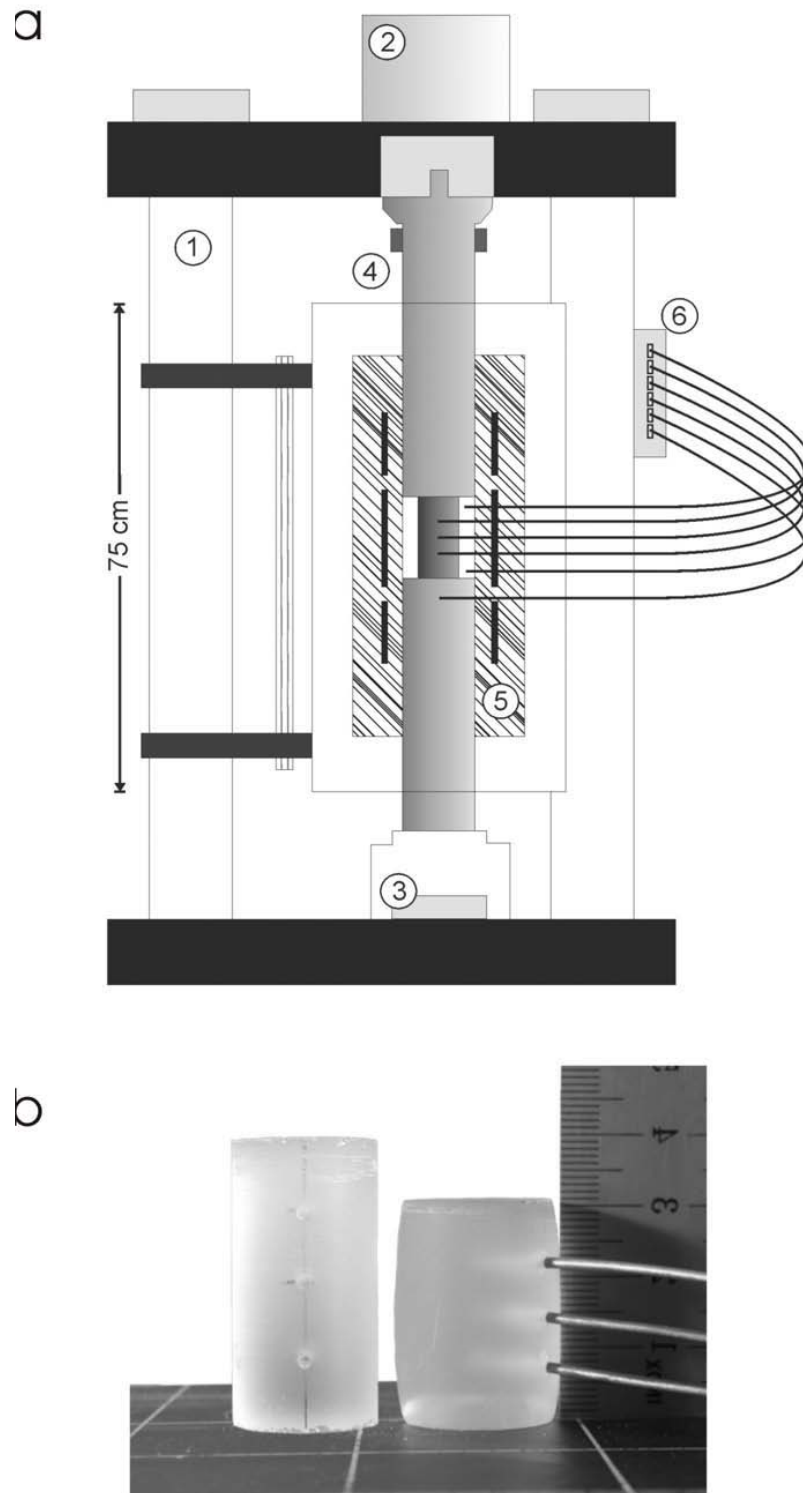
Figure 1.1: (a) Sketch of the uniaxial press: (1) load frame; (2) servo cylinder with LVDT; (3) load cell; (4) cooling jacket; (5) 3-zone split cylinder furnace; and (6) 6-input thermocouple interface (for type K and S). The sample containing three thermocouples is placed between the pistons. Two thermocouples monitor the ambient air and one the piston temperature. (b) Photograph of a NIST 717a sample with three drill holes for thermocouples, alongside a deformed samples inserted by three thermocouples. Modified from *Hess et al.* [2007].

Samples were placed between the pistons and slowly heated up to a fixed temperature (NIST: 540-630 °C, and Obsidian: 685-850 °C). After slow thermal equilibration of the sample and pistons (8 hrs), a high load was applied and maintained until a maximum of 33 % strain was obtained. The resultant length changes (dh) were recorded by the differential transducer (LVDT) at a rate of 10 data per second (dt) which were then treated via Gent equation developed to calculate the shear viscosity (η_s in Pa*s) of a cylindrical melt in parallel-plate compression measurements (Gent, 1960):

$$\eta_s = \frac{2\Pi F h^5}{3V \frac{dh}{dt} \left(2\Pi h^3 + v\right)} \tag{1.2}$$

where F is the force (N), h is the length (m), and V is the volume of melt (m^3). Temperature changes produced by the deformation work were measured in situ during the experiment; the ambient temperature was maintained during deformation and the measured temperature increase of the melt could be purely attributed to viscous dissipation. For the NIST 717a glass, we used the measured mean sample temperature (T_{mean} see Table 1.2) to estimate the viscosity and compare it to the measured viscosity. Below we show that, with this experiment, we have achieved the first in situ experimental confirmation of viscous heating during high temperature, high stress deformation of dome lava.

Table 2. Experimental results and calculated viscosities for the NIST reference material SRM 717a.
T_{mean} was obtained by averaging the recorded temperatures of all three thermocouples inside the samples.

Sample		Stress (MPa)	Strain (%)	Strain Rate (s^{-1})	Log measured viscosity (Pa·s)	T_{mean} (°C)	Log calculated viscosity (Pa·s)
VH1	initial	46	0.0	1.6E-02	8.98	614.1	8.95
	end	46	19.4	1.3E-02	8.93	617.0	8.87
VH3	intial	73	0.0	2.3E-02	8.99	611.1	9.03
	end	73	21.4	2.1E-02	8.84	617.2	8.86
VH4	intial	110	0.0	4.0E-02	8.94	611.4	9.02
	end	110	17.3	6.4E-02	8.71	621.7	8.74
VH6	intial	81	0.0	1.1E-04	11.31	540.4	11.39
	end	81	1.6	1.3E-04	11.32	540.0	11.40
VH6	intial	120	1.6	1.9E-04	11.29	540.1	11.40
	end	120	4.7	1.5E-04	11.31	539.4	11.42
VH7	intial	78	0.0	1.3E-03	10.27	570.1	10.29
	end	78	11.3	1.2E-03	10.25	570.2	10.29
VH9	intial	140	0.0	3.1E-02	9.16	605.1	9.20
	end	140	13.5	4.1E-02	8.95	614.0	8.95
VH10	intial	27	0.0	2.3E-02	8.58	627.1	8.60
	end	27	10.0	2.2E-02	8.55	628.3	8.57
VH11	intial	28	0.0	2.3E-03	9.59	588.6	9.69
	end	28	14.1	1.9E-03	9.59	587.9	9.71
VH13	intial	55	0.0	6.0E-03	9.49	593.6	9.54
	end	55	19.2	5.0E-03	9.41	596.4	9.45
VH14	intial	50	0.0	6.0E-03	9.43	599.8	9.35
	end	50	22.9	4.8E-03	9.33	601.2	9.31
VH19	intial	130	0.0	8.6E-03	9.69	591.3	9.61
	end	130	21.6	1.2E-02	9.42	599.7	9.36

Table 1.2: Experimental results and calculated viscosities for the NIST reference material SRM 717a. T_{mean} was obtained by averaging the recorded temperatures of all three thermocouples inside the samples.
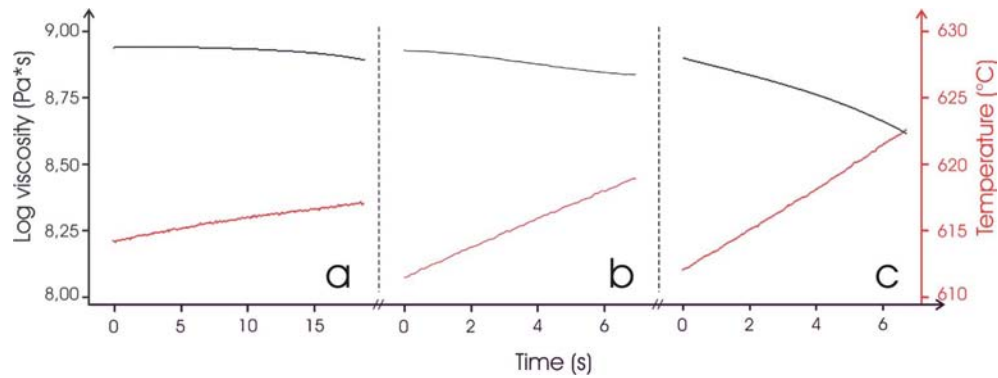
Figure 1.2: Temporal profiles for three experiments showing the viscosity decrease (line) and associated temperature increase (doted lines) of viscous dissipation. Experiments with (a) 46 MPa, (b) 73 MPa, and (c) 110 MPa of applied stress.

1.3   Results

22 measurements were performed on the NIST glass to quantify as broadly as possible the effects of viscous dissipation on the rheology of silicate melts (Table 1.2). A typical low-stress, or low-strain-rate, experiment is characterized by a derived viscosity which initially increases at a decreasing rate then stabilizes to a steady value. The temperature recorded by the embedded thermocouples remained constant throughout low-stress experiments. In contrast, medium- to high-stress experiments reveal an accentuating decrease in viscosity accompanied by an internally recorded temperature increase of up to 10 °C (Figure 1.3).

Table 3. Experimental results for Iceland obsidians.
T_{mean} was obtained by averaging the recorded temperatures of all three thermocouples inside the samples.

Sample		Stress (MPa)	Strain (%)	Strain Rate (s^{-1})	Log measured viscosity (Pa·s)	T_{mean} (°C)
Ice3	intial	100	0	3.3E-04	11.08	740.2
	end	100	10.8	3.3E-04	11.08	740.4
Ice4	intial	74	0	2.0E-02	9.08	840.3
	end	74	20.9	1.9E-02	8.98	849.1
Ice5	intial	77	0	2.2E-03	10.05	793.4
	end	77	24.9	2.1E-03	9.94	799.7
Ice6	intial	129	0	3.9E-03	10.02	794.6
	end	129	22.3	5.6E-03	9.74	807.4
Ice7	intial	120	0	4.5E-03	9.92	797.3
	end	120	12.3	6.8E-03	9.67	806.3

Table 1.3: Experimental results for Iceland obsidians. T_{mean} was obtained by averaging the recorded temperatures of all three thermocouples inside the samples.

The temperature increase generated during deformation of NIST reference melts correlates positively with the strain rate (Figure 1.3). The deformation of natural rhyolitic melts produced a similar temperature increase (Table 1.3).
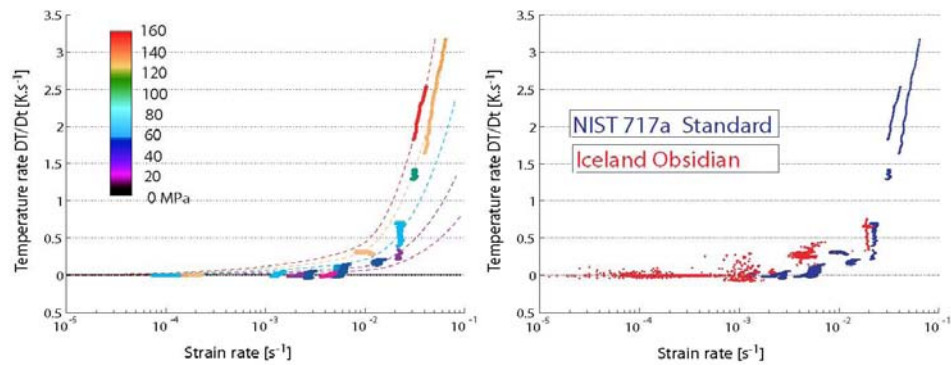
Figure 1.3: Production rate of temperature versus strain rate and applied stress (colour coding). (a) Experiments for the SRM 717a glass. The coloured dotted curves show the trend correlating with the measured heating rate according to the experimental strain rate. (b) Comparison between the SRM 717a glass (blue) and an icelandic obsidian (red).

In particular, the rate of heating shows a pronounced increase as the strain rate approaches $10^{-3}\,\mathrm{s}^{-1}$. During the experiments most temperature changes appear to be attributed to viscous heating and conductive dissipation of heat out of the sample to the surrounding ambient air was not recorded by the thermocouples around the samples.
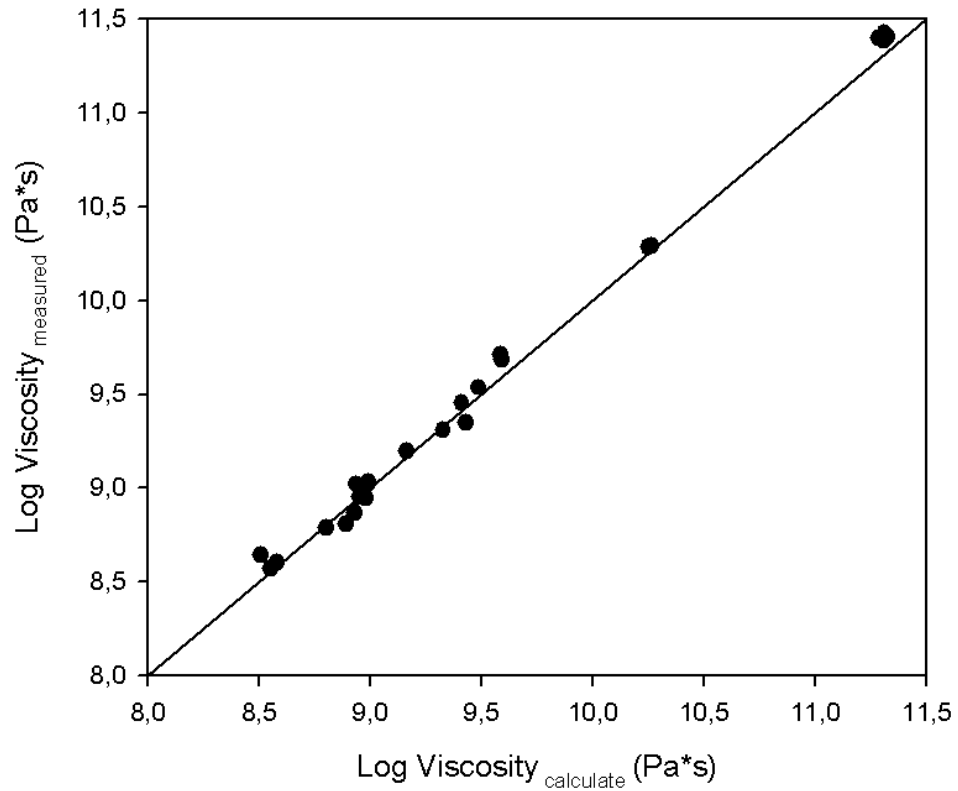
Figure 1.4: Comparison between the measured values and calculated values of viscosities (based on T_{mean}) for the SRM 717a glass composition.

The apparent Newtonian viscosity derived from the experimental data may differ significantly from the viscosity anticipated using the nominal or external experimental temperature. Thus the internal sample temperature (T_{mean}) was used to calculate the viscosity (applying the Fulcher equation from the NIST certificate), and then compared to the experimental viscosity (Figure 1.3).

Correction for viscous heating using this approach completely accounts for the apparent drop in viscosity. During all measurements, the precisions of the measured viscosity changes remained within 0.06 logarithmic unit of the calculated viscosity changes (in Pa*s) independent of the conditions of applied stress, strain rate, and recorded heating (Figure 1.3). The observed viscosity decreases in these experiments could be therefore attributed entirely to viscous heating.
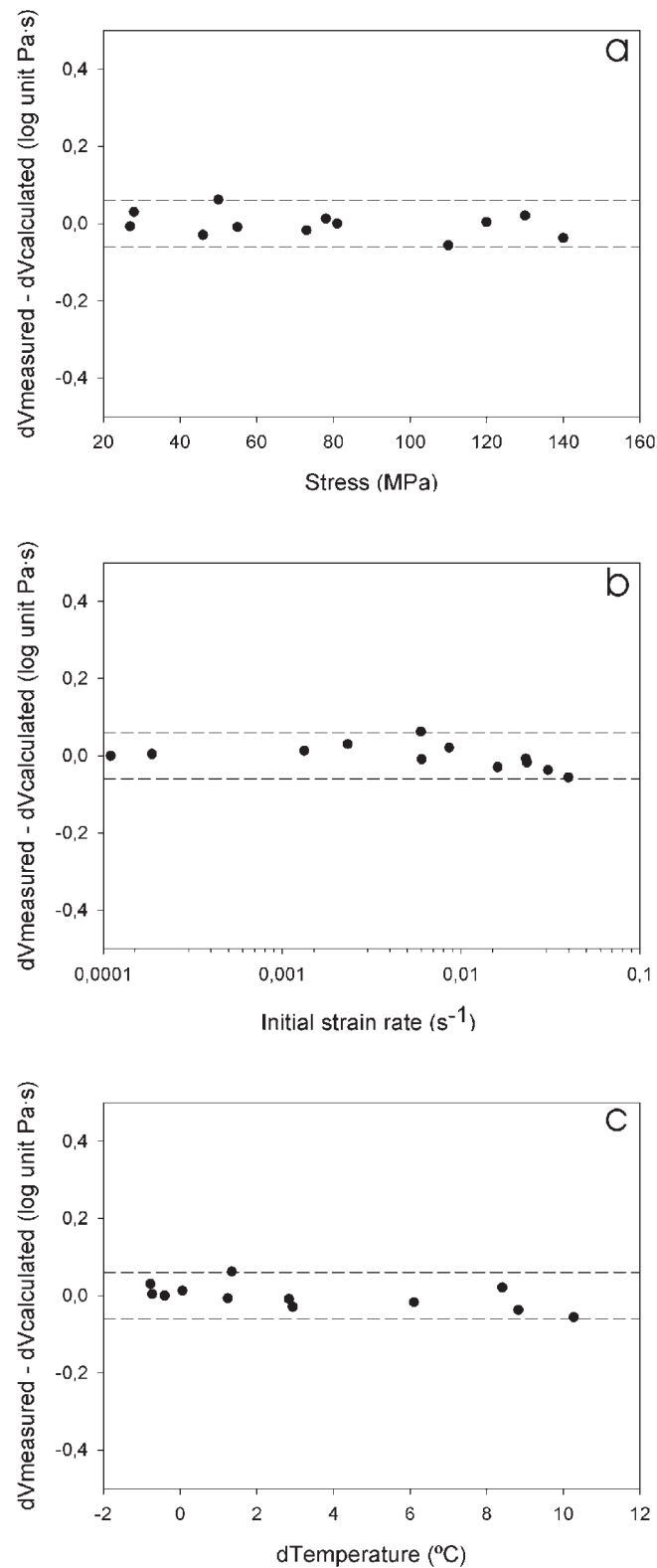
Figure 1.5: Differences between the variations of measured viscosity and the calculated (certified) viscosity variations against (a) stress (b) temperature, and (3) strain rate. The dotted line denotes the precision of the measurement equal to 0.06 logarithmic unit in Pa*s. The absence of a preferential dependence to stress, temperature, or strain rate indicates that viscous heating could be the sole detectable cause of non-Newtonian behaviour in these experiments

1.4   Interpretation

The heat generated during energy dissipation correlates positively with the strain rate. We have observed that the heating rate shows a pronounced increase when approaching 10^{-3} s^{-1} (Figure 1.3). Note that this strain-rate records the measurement of significant viscous heating in these experiments and not its theoretical onset. Presumably, at lower strain rates, heat is generated at too low a rate to overcome heat loss by conduction, thus excluding the observation of viscous dissipation effects. This balance of heat (in and out of the sample) is classically understood in fluids dynamic as the viscous heating efficiency defined by the dimensionless numbers of Brinkman or Nahme (Na). Na represents the ratio between the heat gained by viscous heating and the heat loss by conduction, so that value greater than one would imply that temperature increases as a result of viscous heating. In a first approximation, Na can be expressed as:

$$Na = \frac{\sigma \dot{\gamma} A}{\kappa dT} \tag{1.3}$$

where σ is the applied stress, $\dot{\gamma}$ is the strain rate, A is the area, κ is the thermal conductivity, and dT is the temperature gradient from the centre of the sample to the end. We can rewrite this equation to express the strain rate at which viscous heating becomes experimentally important, to:

$$\dot{\gamma} = \frac{Na \kappa dT}{\sigma A} \tag{1.4}$$

For experiments on NIST 717a melt (A= 0.0314 m^2 and κ= 1.3 Wm^{-1}K^{-1} based on in situ thermal diffusivity, heat capacity and density measurements), we measure an onset of viscous heating (i.e., if a dT¿0 K, then Na≥1) at applied stresses

greater than 20 MPa, which correspond to a strain rate higher than 10^{-3} s^{-1}. This value is in good agreement with our observation in Figure 1.3. The viscous heating production rate is proportional to the tensorial product of stress and strain rate. Here, neglecting heat conduction term, we simplify the production rate of viscous dissipation (dT/dt) to:

$$\frac{dT}{dt} = \frac{\sigma\dot{\gamma}}{\rho Cp} \tag{1.5}$$

where σ is the applied stress, ρ the density, and Cp the heat capacity of the melt. Since the stress applied on a viscous fluid equals the product of viscosity (η) and strain rate, equation 1.5 can be reduced to:

$$\frac{dT}{dt} = \frac{\eta\dot{\gamma}^2}{\rho Cp} \tag{1.6}$$

This formulation provides a first order explanation for the non-linear increase of heating rate observed in our experiment. It also yields an equivalence of behaviour between the NIST glass and the natural rhyolitic melts (Figure 1.3). This relationship, theoretically anticipated and confirmed by the present results, may have profound consequences for magma ascent and the transition to high-discharge rates during eruption (e.g. *Costa and Macedonio* [2003a]; *Costa* [2005]; *Mastin* [2005a]; *Vedeneeva et al.* [2005]; *Costa et al.* [2007]).

1.5   Viscous heating in the glass transition.

When the strain rate of silicate melt deformation approaches the timescale of structural relaxation, the melt can no longer behave as a Newtonian fluid. In experiments involving significant strain, such melts exhibit strain-rate dependent viscosity (shear thinning) until they fail macroscopically [*Simmons et al.* 1982a; *Webb and Dingwell* 1990a].

Previous rheological works on the onset of non-Newtonian rheology in geological melts have not incorporated in situ monitoring of the sample temperature. The early work on fiber elongation provided a simple parameterization of heat loss to argue for an absence of viscous heating effects from those thin fibers [*Webb and Dingwell* 1990a]; postulating at the same time that the high-torque concentric cylinder work of Stein und Spera [*Stein and Spera* 1992] might have been influenced by viscous heating. Yue and Bruckner [*Yue and Brckner* 1994] later re analysed the parallel-plate and fiber-elongation observations and formulated a correction for the strain-rate dependence of viscosity that includes viscous heating effects explicitly. The question as to whether viscous heating may have had a measurable effect on previous determinations of the onset of non-Newtonian viscosity remains. We cannot say explicitly because the sample geometries, stresses and strain-rates have been very different in the experiments to date.

We can however reiterate two important observations. Firstly, the onset of non-Newtonian viscosity appears to arrive earlier (approximately three orders of magnitude) than theoretical prediction based on linear stress-strain approximations (the Maxwell model) [*Webb and Dingwell* 1990a]. That might imply a contribution of viscous heating. Secondly however, the onset of non-Newtonian rheology has always been recorded at approximately three orders of magnitude

before the predicted strain rate of the structural relaxation time for experiments performed under compression, simple shear and elongation, and for devices operating on very different sample thermal masses, viscosities and strain rates [*Simmons et al.* 1982b, 1988; *Webb and Dingwell* 1990a]. That observation might imply that viscous effects are not significant at the onset. In any event, viscous dissipation alone cannot explain the subsequent failure of samples which have been forced into non-Newtonian deformation.

In volcanic conduits, slow ascent rates likely yield low shear rates (e.g., $<10^{-3}$ s^{-1}), negligible viscous dissipation, and simple Newtonian response of the liquid. At higher strain rates (e.g., $>10^{-3}$ s^{-1}), or upon strain localization along the conduit margin, viscous heating may become a primary rheological control. It has been proposed that viscosity reduction by viscous heating moves the magma away from the glass transition despite increasing shear rates. [*Gonnermann and Manga* 2007]. Yet textural analyses in pumices have been interpreted as evidence for the occurrence of viscous heating before brittle deformation [*Rosi et al.* 2004; *Polacci* 2005]. Viscous heating does serve to decrease the viscosity, but there may be thermal - fluid dynamic scenarios whereby the viscously heated magma can leak its heat more rapidly such that the rapidly deforming magma may fail even more effectively than in the absence of a viscous heating history [*Dingwell* 1996]. During laminar flow (e.g. *Mastin* [2005a]) we suggest that lava flow would not be incompressible and steady as viscous heating would thin the magma along the conduit margin and drive magma ascent. This chain of reactions may be common inside volcanoes, especially for medium to high viscosity magmas (10^4 to 10^{12} Pas) as viscous heating may either accompany or immediately succeed the onset of structural non-Newtonian rheology.

1.6   Conclusion

Parallel plate experiments have been conducted to characterise the effects of the viscous dissipation on high-viscosity magmas. Viscous heating is observed to be strain-rate dependent and becomes rheologically significant, at these viscosities, above approximately 10^{-3} s-1. Simple analysis shows that the temperature generated through viscous deformation in the experiments could be the sole cause of apparent non-Newtonian rheology in these experiments. Once the temperature generated is accounted for in the construction of the viscosity-temperature relationship, the rheology is consistent with a Newtonian regime. The interplay of viscous heating and structural onset of non-Newtonian rheology is likely to control the ascent of highly viscous magmas in manner which is not yet fully understood and whose understanding would undoubtedly be enhanced by systematic controlled deformation experiments with the capability for viscous heating monitoring.

Chapter 2

Viscous heating, non-Newtonian and Brittle onset: An energy interaction

> *"...a pile of stones is not a house and a collection of facts is not necessarily science."*

Henri Poincaré

> *"All science is either physics or stamp collecting."*

Ernest Rutherford

... were the both motivations of this chapter.

Here we re-examine the results obtained in chapter 1 and bring a new light thanks to numerical simulations. The strength of this approach is that we completely constrain this model via the calibration of the press performed during the first year of this study. Moreover, the material investigated has been measured by a battery of tests and the full analytical power of this department. Optical observations, chemical measurements, dilatometry and laser flash methods offered all the parameters needed to obtain accurate numerical simulations able to reproduce our experimental results.

Consequently, we can use at our numerical simulations to interpret the experimental phenomena observed. This interpretation gives new hints for more generalised geological simulations dealing with volcanic conduits, subductions or orogens processes. We hope to obtain a new view on volcanoes and mountains. Consequently, this is a wonder journey between reality and numerical simulations, from the small to large scales.

More specifically, this chapter reveals the importance of all the terms in the energy equation. Historically, geology has tested many non-Newtonian laws to explain the dynamics observed. Most of them are derived from the polymer industry.

If polymers clearly have complex structural behaviour, here we demonstrate that by simply 'switching on' the viscous heating, we can answer to most of the non-linear dynamical effects observed in pure silicate liquids. If viscous heating results in non-linear dynamics, it has the elegance to give a simple explanation to the observed phenomena. Another results is that viscous heating appears to be a parameter for the brittle onset. It may consequently open a door to a new brittle-ductile transition theory.

2.1 Introduction

The viscous heating effect is to fluids what fracturing/cracking is to solids: an efficient way to release excess energy input. When a force is applied to a fluid, it deforms because of the work transferred to the inner energy of the system. Thus, part of the work energy is stored by the elastic term while all the rest is dissipated and used by the deformation process. Deformation generate friction in the fluid plains which dissipates all thermally: the liquid heats up. As most of Earth material can be assumed visco-elastic this effect appears as the most relevant for Earth dynamics [*Burg and Gerya* 2005, and references therein].

Any system with a thermo-dependent viscosity will see its dynamics affected by viscous heating. This is a first order parameter in the conservation energy equation. However from a geological point of view this term is often neglected for the sake of simplification. Many justifications are commonly involved (1) Geological evidence is no more than fragmentary; (2) Heat conduction is too fast; (2) Viscous heating is self-destructive for a constant strain rate; (3) Viscous heating is only local around shear zones and has no regional significance; (4) Fluids infiltrating along shear zones carry the heat away [*Burg and Gerya* 2005].

For those reasons the viscous heating is often 'switched off' in earth science flow dynamics. However no real studies have justified this approximation while many papers have discussed and proved experimentally or numerically the potential of this term.

Despite the early work of Schubert & Yuen [*Schubert and Yuen* 1978] and many complementary publications [*Larsen et al.* 1995; *Bercovici* 1998], concerning the mantle dynamics debate, viscous heating is still poorly accepted by the geological community. Moreover viscous heating seems to affect many other geo-

logical processes such as in subduction zones, it gives some 'fuel' to an unexpected phenomenon: the 'cold plumes', compositionally initiated and propagated thanks to the self lubrification generated by viscous heat [*Gerya and Yuen* 2003]. Moreover viscous heating also has its importance in plate tectonics [*Platt and England* 1994; *Schott et al.* 1999]. Finally it is also known that the viscous heating affects mountains orogens as it can cause a localisation of the deformation. The heat production generated from this process is comparable or even exceeds the radiogenic production of the crust [*Burg and Gerya* 2005; *Burg and Schmalholz* 2008; *Hartz and Podladchikov* 2008].

An other major geologic and highly dynamic system subject to viscous heating effects are volcanic processes. Either the lava emplacement or the magmatic conduit is affected by self heating. *Booth and Self* [1973] were the first to suggest a viscous heating through the roller vortex of spreading lavas. Moreover thermal erosion of lavas mechanisms observed on the field is often observed for highly dynamic lava flows [*Greeley et al.* 1998]. Measurements performed on basal lava flows first recorded a drastic cooling unexpectedly followed by a temperature increase [*Keszthelyi* 1995b]. *Keszthelyi* [1995c] suggested that if viscous heating is here not the single parameter involved in the energy budget; it remains that a dynamic process is not only led by the conductive heat loss but an intimate interaction of the energy loss and gained [*Keszthelyi* 1995c]. Numerical investigations on the effect of viscous heating effect on lava flows were performed and reported by *Costa and Macedonio* [2003b].

Volcanologists also investigated the potential effect in the conduit flow. Most of those surveys suggested a self lubrication of the conduit walls triggering to an increase of the magma velocity [*Mastin* 2005b; *Costa and Macedonio* 2005; *Hale*

and Muhlhaus 2007]. From a field evidence this process has been suggested for the Pinatubo eruption [*Polacci et al.* 2001].

If the viscous heating effect is hardly measured in the field, it has been experimentally and numerically largely investigated in rheological measurements [*Gallop* 1955; *Turian and Bird* 1963; *Turian* 1965; *Kearsley* 1962; *Papathanasiou et al.* 1997; *Calado et al.* 2005], metallic industry [*Nishiyama and Inoue* 1999; *Kato et al.* 2003, 2006, 2007] and silicate melts [*Hess et al.* 1995]. Numerically it produced interesting outcomes and interpretations and shows that this is a topic still in progress [*Becker and Mkinley* 2000; *White and Muller* 2000b, 2002a,b; *Avci and Aydin* 2008; *Coelho and Pinhoa* 2009].

Thus, neglecting the viscous heating effect may be a correct approximation for quasi static processes where the heat transfer overcomes by many orders of magnitude the heat production. However, and for most of the dynamic cases, viscous heating will produce enough energy to modify the dynamic of the system itself. Therefore, for earth processes for which the shear heating contribution is unknown or not well understood, the approach is to include it and show its pertinence rather than ignoring it as a priory unimportant effect.

For the first time we have the opportunity of bringing together 1) an experimental press with a sufficient size that allows to work on hot and big samples; 2) two methods of measuring the viscous heating effect, directly with 'in situ' thermocouples and indirectly through viscosity measurements where the temperature dependence is well known; 3) a numerical code that bring us a direct 'vizu' of the stresses, temperatures, viscosities and the strain-rates in our sample.

2.2 Methods

In order to constrain the viscous heating effect we conducted both experimental and numerical tests.

2.2.1 Experimental

The experimental viscosity measurements were performed with a high load, high temperature uni-axial press [*Hess et al.* 2007].

The material used in this survey is the SRM 717a an homogeneous silicate glass certified by the National Institute of Standards & technologies. The viscosity (η) of this material has been measured independently by seven laboratories and its dependency with temperature can be obtained through the following Flucher equation [*Hess et al.* 2007]:

$$\log_{10}(\eta) = -2.5602 + \frac{4852.2}{T - 192.462} \tag{2.1}$$

T is here the temperature in °C.

Cylindrical samples 40 mm high and 20 mm wide were prepared and three holes of 2-mm diameter, equally spaced along the samples axis, were radially drilled through to the centre. Three thermocouples were inserted for precise monitoring of the temperature variation during the experiments. Samples were placed between the pistons and slowly heated up to a fixed temperature. After a slow thermal equilibration of the sample and pistons (8 hours), a load was applied and maintained upon a maximum of 30% strain.

The data were treated and the viscosity calculated through the Gent equation [*Gent* 1960]:

$$\eta_a = \frac{2\pi F h^5}{3V \frac{dh}{dt}(2\pi h^3 + V)} \tag{2.2}$$

With η_a the apparent viscosity [Pa.s], F the applied load [N], h the distance between the parallel plates [m], V the volume of the sample [m^3], and t the time [s].

The thermal parameters such as density, specific heat and thermal conductivity have been respectively measured from the samples through dilatometric, differential scanning calorimetry, and laser flash methods (see Fig. 2.1). Those measurements have been performed from room temperature to 620°C above the glass transition of the material here obtained at 550°C (the onset being around 495°C). Above this temperature the thermal parameters are considered constant as we enter the super cooled liquid state.

Please note that literature does not have measurements for this particular composition in the super cooled liquid range. The thermal conductivity is calculated from the relation between the diffusivity, the density and the heat capacity. The heat capacity and the thermal diffusity can be, with a good approximation, assumed constant in the supercooled liquid range. Nevertheless this is not the case of the density.
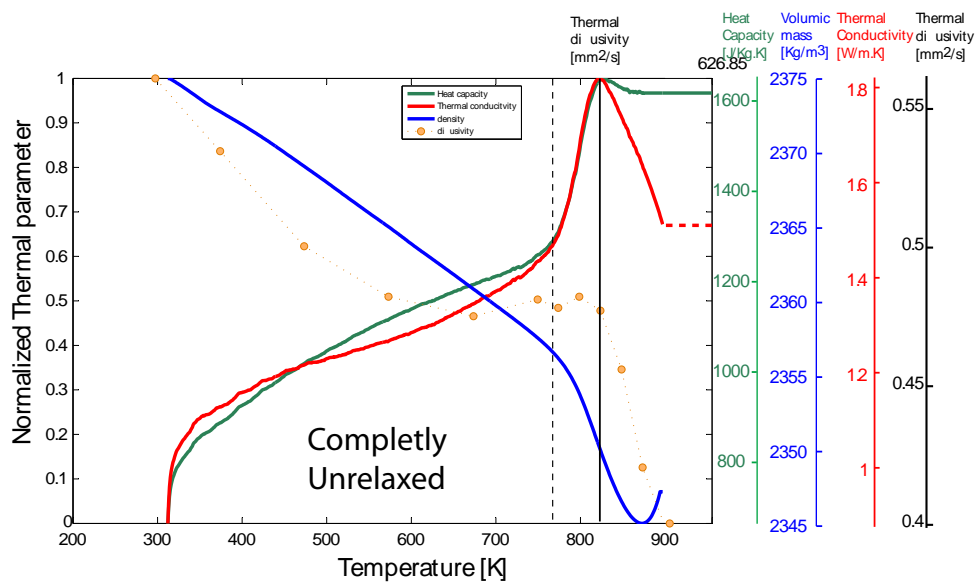
Figure 2.1: Thermal parameters of the SRM NIST 717a. We can observe a glass transition temperature around 550°C (vertical solid line) with an onset around 495°C (vertical dashed line). The inflexion point is about 525°C.

Few surveys investigated this domain and proposed a model [*Knoche et al.* 1995; *Gottsmann and Dingwell* 2000; *Potuzak and Dingwell* 2006]. A first approximation would be to extrapolate the solid curve and fix it as an upper limit. However *Gottsmann and Dingwell* [2000] performed measurements with a unique container based dilatometry on NIST glass 710. It shows that the thermal expansivity of the glass increase by three in the supercooled liquid range. Our measurements appears to be within this range and without more constrains, we decided to keep the data measured as the ones used for the model.

The experiments are spanning a range of 530°C to 560°C. We are consequently working in the classical glass transition range of fluids. From a physical point of view, this is not so much the temperature range that matters here but more the viscosities investigated and their related structural relaxation timescale. Part of the experiments have already been published [*Hess et al.* 2008]. However we performed a new set of experiments, three were to confirm the first observations at a constant load and ten at constant velocities. We investigated constant velocity experiments because this boundary condition is known to cause a self destruction of the viscous heating process as the heat production will always decrease with time [*Brun and Cobbold* 1980; *Kameyama et al.* 1997, 1999; *Kameyama and Kaneda* 2002; *Kaus and Podladchikov* 2006].

2.2.2 Numeric

Subdomain

The numerical simulations presented here are based on the geometry described in figure 2.2. In a axis-symmetric approximation of the sample, we resolve the
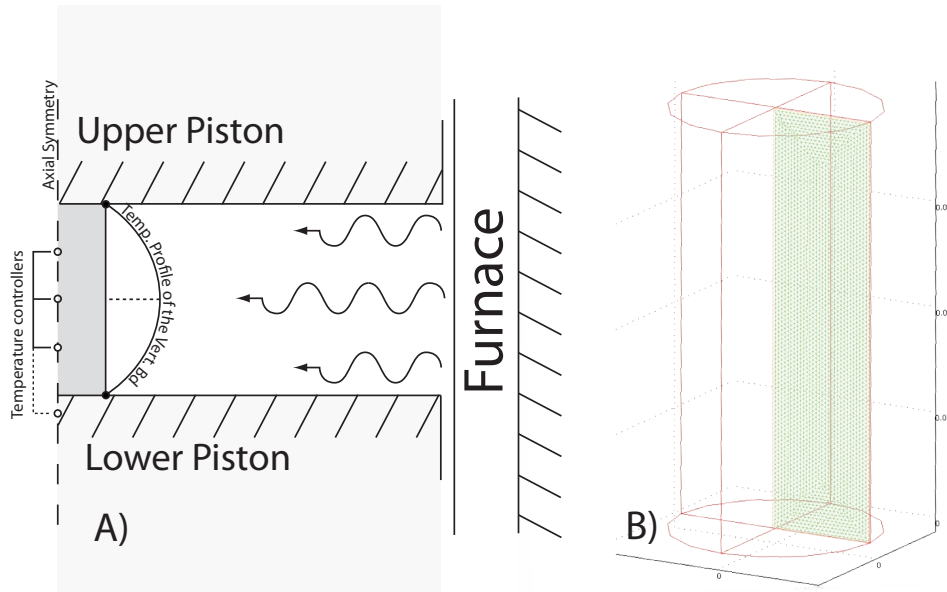
Figure 2.2: A) Schematic view of the parallel plate method. The experimental method consists in a cylindrical sample placed between two pistons. The sample is homogeneously heated up by the surrounding furnace.The temperature evolution is recorded within the sample but also at the contact in the lower piston. B) Structure of the numerical simulations. With an axis symmetric assumption the mesh is reduced to a half section of the cylinder.The temperature conditions are defined by the measurements made during the experiments (see Appendix A section 2.6).

classic navier-stokes equation set. Consequently our experimental samples are

simply defined through a rectangular section of the cylinder.

We use here a simple and pure viscous approximation and the momentum equation can be written the following way:

$$\rho \frac{\partial \mathbf{v}}{\partial \mathbf{t}} + \rho(\mathbf{v} \cdot \nabla)\mathbf{v} = \nabla \cdot (-pI + \eta(\nabla \mathbf{v} + (\nabla \mathbf{v})^T)) + \mathbf{F} \qquad (2.3)$$

With ρ the volumic mass [kg.m^{-3}],t the time [s], v the velocity field [m.s^{-1}], η the dynamic viscosity [Pa.s] and F the volume body forces (as we neglect gravity effects this term is null).

We assume an incompressible fluid leading from the continuity equation to:

$$\nabla \cdot \mathbf{v} = \mathbf{0} \qquad (2.4)$$

The balance of energy between the heat produced (Φ_g) and the heat loss (Φ_l) is solved the following way:

$$\rho \frac{\partial u}{\partial t} = \Phi_g - \Phi_l = \sigma \overline{\overline{\otimes}} D - \nabla \cdot \mathbf{q} \qquad (2.5)$$

The left hand side is the volumic inner energy variation [W.m^{-3}], σ the stress tensor [Pa], D the strain rate tensor [s^{-1}] (i.e. the symmetric part of the velociy gradient) and q the heat flux [W.m^{-2}].

The first member on the right hand side of the equation is called the inverse of the volumic density of mechanical power of the inner stress. Integrated over time it gives the energy used for the deformation of the volume considered. While relaxing the stress the deformation dissipates energy to reach a lower equilibrium level. In a pure viscous approximation all this energy is thermally transformed

through the friction of the fluid plains. It consequently represents the viscous heating term. Assuming a perfectly viscous body, we have $\sigma = 2*\eta D + (\Lambda Tr(D) - p)I$. Equation 2.3 allows us to neglect the mechanical stress of pressure and the small deformation approximation leads us finally to:

$$\Phi_g = \frac{\eta}{2}\left((\nabla\mathbf{v} +^t \nabla\mathbf{v})(\nabla\mathbf{v} +^t \nabla\mathbf{v})\right) \tag{2.6}$$

With ϕ_g is the power of the viscous heating [W.m^{-3}].

The solution is solved with a commercial code: COMSOL-Multiphysics. However the problem has been compared to an independant 3D model using equations as developed in *Jaworski and Detlaf* [1972] or *Garrigues* [2007] to implement the viscous heating. However due to calculation time and detailed resolution constrains the 2D asymmetric solution of COMSOL was preferred. Both solutions give similar results.

Boundaries

No relevant radius increases have been observed after experiments on the sample end members; consequently the boundaries in contact with the pistons were set under no slip conditions. The cylindrical surface is an open boundary.

Concerning the temperature boundaries, our goal is to use the temperature conditions that will offer the smallest viscous heating effect as possible. Thus we used the first specie boundary condition of Dirichlet. The uppermost boundary was fixed to the temperature recorded from the piston.

Moreover, the temperature recorded within the pistons of our apparatus exhibit a slight increase in temperature during the most dynamic experiments.

This is suggestive of a transfer of the sample heat to the piston. Consequently the constant temperature rather than a Neumann condition (constant heat flux) is favoured. Indeed the Neumann boundary condition may store the heat and overestimate the viscous heating effect in our sample as the heat flux, in the experimental reality, will increase once the viscous heating takes place. Concerning the vertical surface boundary, the temperature is slightly more elaborated. the calibration of the press demonstrated that while the piston moves down the temperature of the press chamber cools down. It reflects the effect of the pistons. Colder than the furnace those last ones create a thermal boundary limit that cools down the press chamber when they approach each other (for more details see 2.6:Appendix A). This effect also decrease the temperature of the sample if no viscous heating is recorded. Consequently the temperature profile was set to follow this phenomenon and is defined according to the temperature of the pistons and a variable dependent upon the furnace temperature and the distance between the two pistons (see Fig. 2.2 and 2.6:Appendix A).

All this attention put in understanding the processes and the conditions of deformation of our samples allows us to define a numerical model without any free parameter as it is completely constrained by the experimental conditions.

2.3 Results

Figure 2.3 shows that when a sufficient stress is applied on the sample the thermocouples inserted inside the sample immediately react and record a temperature increase. Because of this there exists a close link between the temperature measured and the intrinsic shear viscosity of the material. Once the viscous heating balances the heat loss, the temperature increase recorded matches with a vis-
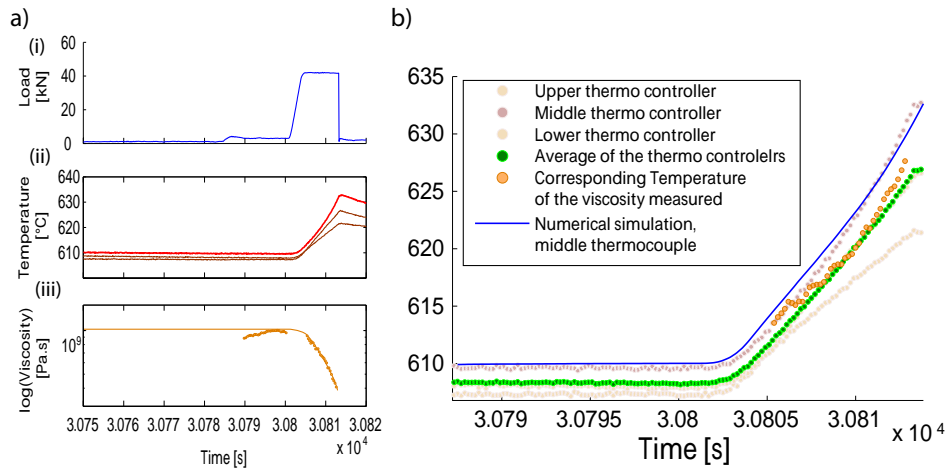
Figure 2.3: Typical experimental sequence. A)(i) A first pressure step is applied to ensure a full contact with the sample. Once the sample relaxed, a high pressure step is applied.(ii) If the pressure is sufficient the temperature recorded in the sample increases. (iii) At the same time the viscosity measured by the press drops.B) Temperatures inside the sample, calculated from the measured viscosity (Eq. 2.1), and the corresponding numerical simulation. One can observe that the average approximation from *Hess et al.* [2007] remains a correct approximation of the phenomenon

cosity decrease measured by the press. The known temperature dependence of the viscosity (see eq. 2.1) allows us to compare the contribution of the viscous heating to the viscosity decrease as exhibited in Fig. 2.3).

Additionally, the corresponding numerical simulation has been plotted and the temperature at the position of the controlling thermocouple has been reported. All of these measurements are in good agreement.Thus we can show to a first approximation that the viscosity decrease measured by the press is mostly due to the temperature increase of the sample itself. Second, the numerical simulation also fit with a good approximation the phenomenon observed during the measurements.

Looking now more globally to the experiments performed compared to the numerical simulations (see Fig. 2.4), we observe that all the experiments exhibit a temperature increase corresponding with the onset predicted by the model. Moreover, the final temperature reached by the experiments is in good agreement with the simulations.

2.3.1   The Temperature rate

Concerning the experimental or the numerical results, both are showing a temperature increase onset above a critical strain-rate between 10^{-3} and 10^{-2} s^{-1}. It represents a dynamic value when the heat production overcomes the heat loss. The system cannot any longer take the heat produced away, thus increasing the temperature. This number is linked to our experimental setup (e.g. dimensions and material used).Consequently it is not specifically representative of what could be met in the field. Indeed, the heat production is dependent on the strain rate, but also on the stress. Consequently the temperature onset may appear in less dynamic systems if the stress is higher, it may also not be visible in extreme dynamic systems if the stress is too low.
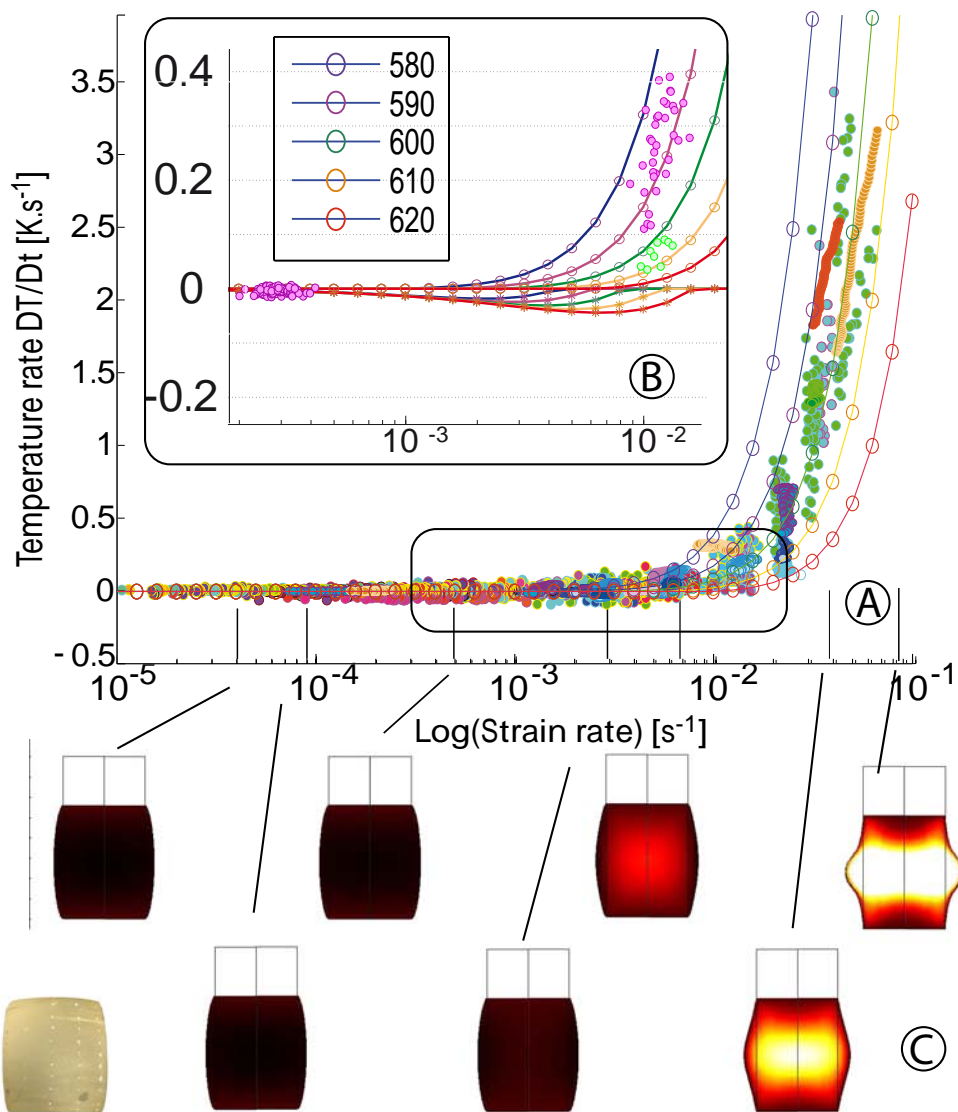
Figure 2.4: A)Temperature rate of the experiments compared to the numerical simulations. We observe an onset of the temperature increase between 10^{-3} and 10^{-2} s^{-1}. B) Span of the onset behavior. The negative values are the transition temperature. During this range, the viscous heating is not strong enough to balance the cooling of the chamber. C) Visualisation of the temperature impact of the viscous heating for different strain rates (T-T$_{t0}$). Initial Temperature 580°C.A real experimental result has been included for comparison

In fig. 2.4.B, we spanned the onset where appears the temperature increase. We left only few experimental points for easy viewing. We observe that in our experiment the viscous heating is not immediately overcoming the heat conduction. The minimum temperature rate (*-symbols) and the maximum (O-symbols) match at the beginning (i.e. extremely low temperature rate decrease) but the most the experiment is fast, the most the temperature rate due to the cooling of the press chamber becomes important and appears in negative values in fig. 2.4.B. However, this phenomenon is for higher strain rates balanced by the viscous heating. During this transition the temperature is first increasing and then decrease due to the cooling of the press chamber. This phenomenon has been largely observed during the experimental part where for those strain-rates the temperature was increasing due to the viscous heating but then was unexpectedly decreasing, sometimes below the initial temperature. The reason being a viscous heating effect unable to balance the cooling of the press chamber. It finds here an explanation and justification why the temperature was decreasing during pressure application for those strain-rates.

Finally, we observe in Fig.2.4.C how much the viscous heating modifies the temperature within the sample. The series of snapshots are all for a strain of 25% and for an initial temperature of 580°C. The plot exhibits the final temperature minus the initial temperature. The variations observed are consequently only due to the viscous heating impact. We see that most of the temperature is generated in the middle of the sample where the shape is highly deformed due to strain localisation.

The temperature rate gives a first estimation of the power gained by the sample minus the power loss.

2.3.2   The importance of the boundary conditions

In our experiments, simulations and even in nature the heat generated and the heat loss are dependent of the thermal parameters and the imposed boundary conditions. The thermal parameters will fix the quantity of energy conducted away (k) or transformed into heat (Cp). The boundary conditions are just as important if not more. The dynamic boundaries (e.g. constant stress-constant velocity-slip or no slip conditions) will define the evolution of the viscous heating. The thermal boundary conditions (e.g. Dirichlet, Neumann or Robin-Fourier) will determine the heat loss. For example a fully insulated system where the heat loss is null will see its temperature increasing immediately after the beginning of the deformation. To sum up the boundary conditions will mostly control the evolution of energy production and loss while the thermal parameters will control the amount produced or lost.

In our experiments the size of our samples does not allow sufficient variations of the thermal parameters to affect the heat generated or lost. To ensure this we performed a simple test. We ran two sets of experiments, one with thermal parameters fixed to the super cooled liquid value, the other one with thermo dependent values as shown in fig. 2.1. Both energy gained and energy loss in the numerical simulations with fixed or temperature dependent thermal parameters overlap. We can thus observe that the effect of the thermal parameters is for the most negligible in our setup (see Fig.2.5).
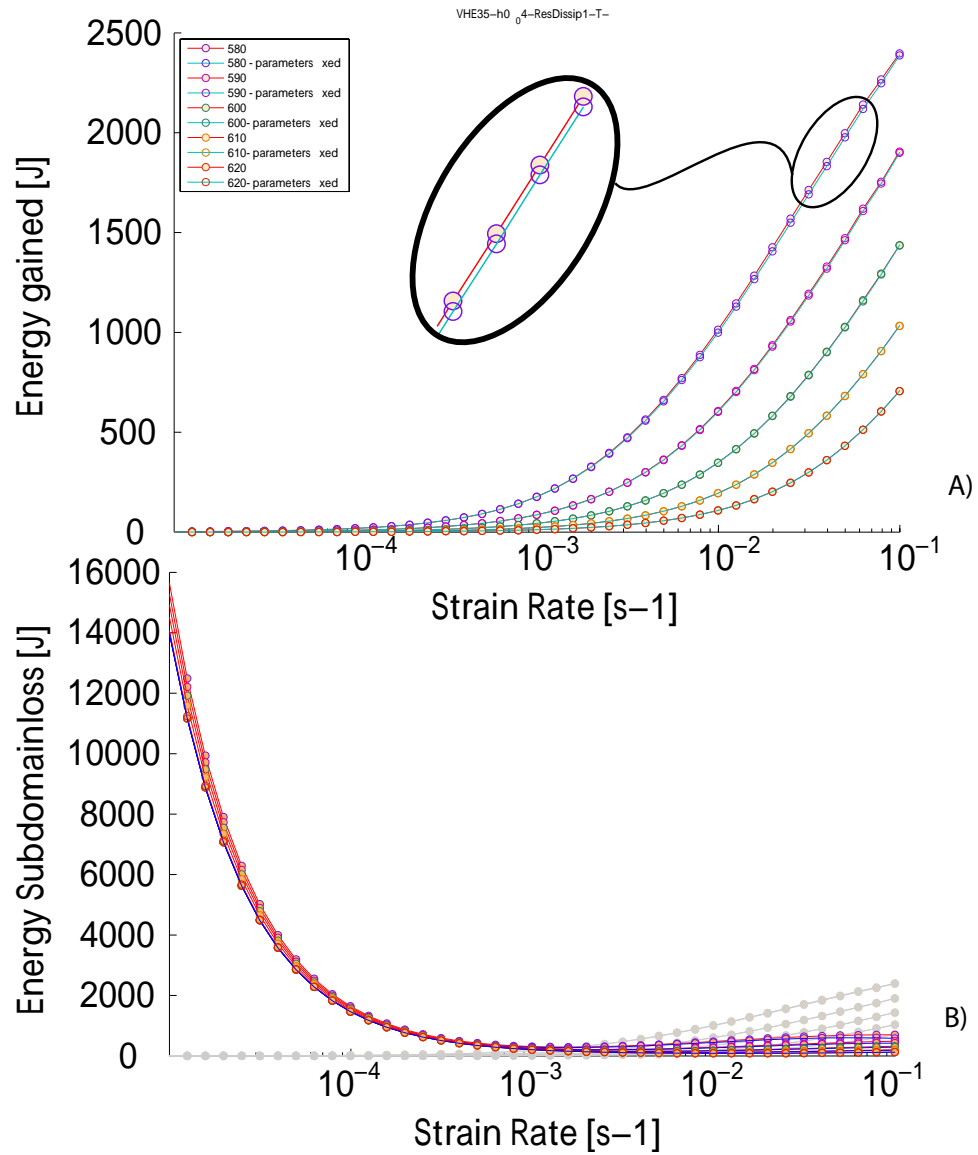
Figure 2.5: Sensitivity of the thermal parameters. Two sets of experiments with fixed or thermodependant parameters are here compared. A)Energy gained B)Energy lost. Notice that the gray plot is the energy gained plotted above, it shows when this last one overcomes the heat loss.

Concerning the boundary effect, the focus was put in the difference between constant stress and constant velocity conditions. For a purely viscous material experiencing viscous heating in a constant stress mode, the power gained will continuously increase with time. Indeed the viscosity decreasing due to the temperature increase and the stress remaining constant, the material will constantly undergo a strain acceleration. This phenomenon is commonly believed to lead to a thermal runaway [*Brun and Cobbold* 1980; *Braeck and Podladchikov* 2007]. On the contrary, constant velocity experiments, by decreasing the viscosity will decrease the stress undergone by the system. Subsequently the power gained will constantly decrease with time. Those two phenomena were perfectly observed in our experiments (see Fig. 2.6.B).
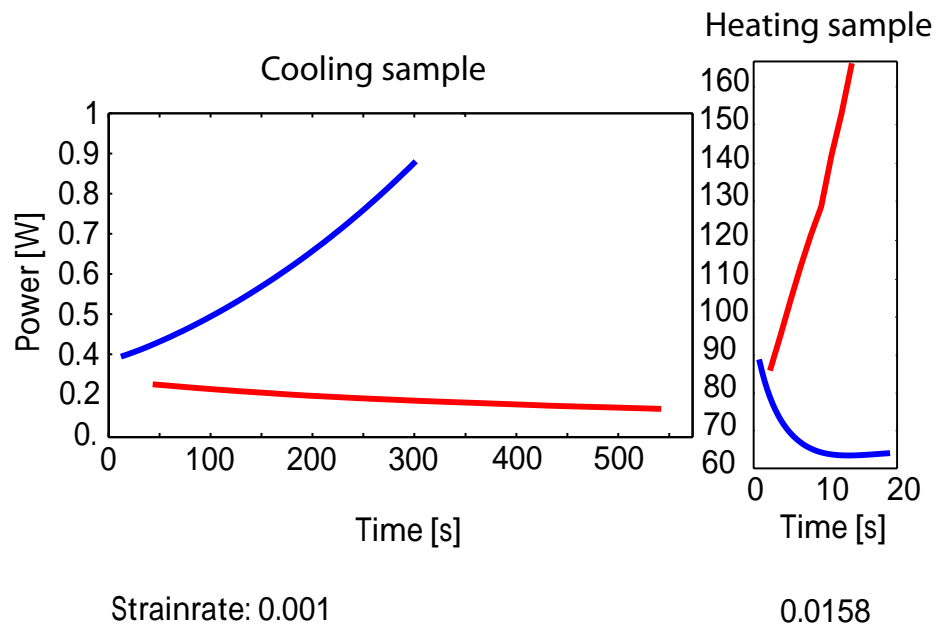
Figure 2.6: Time evolution of the power gained for constant stress (red line) and constant velocity (blue line) conditions. As said above, the cylindrical surface is fixed to follow the process observed with the press. It consequently follow the temperature decrease with the progressive shortening of the sample A)Strain rate is equal to 10^{-3}: The sample is cooling down B)Strain rate is equal to $10^{-1.8}$: The sample is heating up. Accordingly to the sign of the energy loss, the effect on the power gained of the boundary conditions is inverted.

As we mentioned above, we set up the cylindrical surface to follow the chamber temperature decrease. As a consequence our numerical sample follows its experimental alter-ego and cools down at low strain rate where the viscous heating is inefficient. If the self destructive effect or the thermal runaway seems theoretically obvious, an interesting result here is to notice that the opposite effect is also true. A material cooling down will act in a completely opposite way; the viscous heating effect will increase with time for constant velocities and decrease for constant stress (see fig.2.6.A). In our experiments and for both conditions the heat gained seems to switch its behaviour around a strain-rate of 10^{-2}s^{-1} if the initial temperature is 580°C. Above this value, constant stress will exhibit an increase with the time of the energy gained while constant velocities will observe a decrease. This effect may have important impacts on the strain localisation.

2.3.3   Energy Balance

As said above, the temperature effect appears only if the viscous heating can balance the heat loss. A common way to look at this problem is to introduce a dimensionless number of the ratio energy gained/produced over energy loss.This number was defined by *Brinkman* [1950] but its definition may change slightly according to the author. Here we define the Brinkman number the following way:

$$Br = \frac{\phi_g}{\phi_l} = \frac{\sigma \overline{\overline{\otimes}} D}{\Delta(kT)} \tag{2.7}$$

We can immediately notice that the temperature will increase when the absolute value of the Brinkman number is above 1. Below this number value the system can be considered stable and the fluid Newtonian as the heat loss always
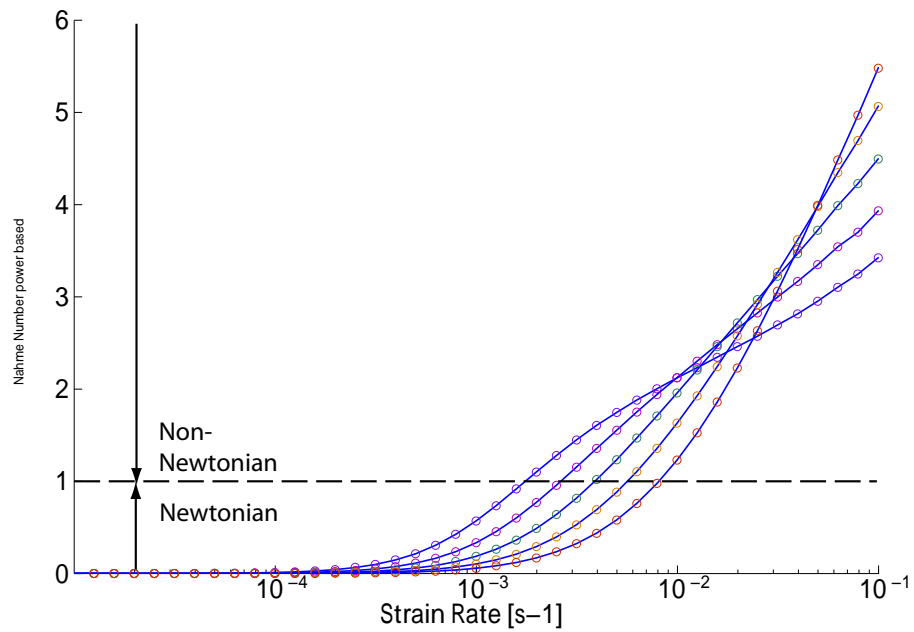
Figure 2.7: Evolution of the Brinkman number in our experiments. A value below one indicates a stable and Newtonian liquid while a value above 1 brings to the Non-Newtonian field.

overcomes the heat production. This number can consequently be seen as the efficiency of the viscous heating effect.

This value can be easily plotted and we can also observe a cross over of the curves. After this cross over area, the lowest temperatures heat slower while they were the first to exhibit a temperature increase onset. The coldest sample exhibits the first temperature increase. However the system exhibit roughly an order of magnitude later a twist. Then the evolution of the Brinkman number is reorganised and the hottest sample demonstrates the highest Brinkman number (it has the most efficient viscous heating efficiency). This singularity is linked to the temperature boundary conditions. For a Dirichlet condition the boundary remains at the same temperature.Consequently when the viscous heating occurs, the heat flux is modified, the temperature gradient becomes higher with time and consequently the heat loss increase. This leads to a decrease of the Brinkman number and the twist observed.

2.3.4   Map & gradients

The viscous heating is commonly believed to generate thermal gradients.Thus a corresponding viscosity gradient may appear. This allows a strain localisation where the viscous heating may even get more pronounced.

In Fig.2.8.A we can observe the temperature gradient within our sample we see that for low strain-rates, the thermal gradient agrees with the thermal conditions defined. However, as the viscous heating effect increases we can observe a strong localisation of gradient on the end members of the sample. This is logical until we realise that the boundary of the end members is the lowest temperature. However we can also observe an inversion of the conduction towards the cylindrical surface. This phenomenon will increase and grow and the gradient will maximise. In our experiments we easily generate at this strain-rates tensile cracks never observed in lower strain-rates (see Fig.2.8.B). Moreover, we observe that the temperature

gradient map completely changes of shape and espouse an inverted map of the von Mises stress (commonly believed to be the cracking indicator). This shape variation seems also to be observed in our experiments (see Fig.2.8.B).This shape modification is due to a strain localisation in the middle of our sample. It increases significantly the vorticity of our samples which may favour the apparition of cracks in the outer middle part of the sample. If we go further, the temperature gradient becomes more homogeneous but keep this relation with the map of the von-Miss stresses. At such strain-rate the sample starts to crack in the press and complete failure occurs relatively fast(see Fig.2.8.B). Here we speculate that the strain localisation observed here has important effect on the dynamic of our sample, change the free surface and leads to the brittle onset. The viscous heating effect can consequently be linked to the brittle behaviour due to strain localisation but also by shaping the thermal gradients to the high stress and future fracturing areas.
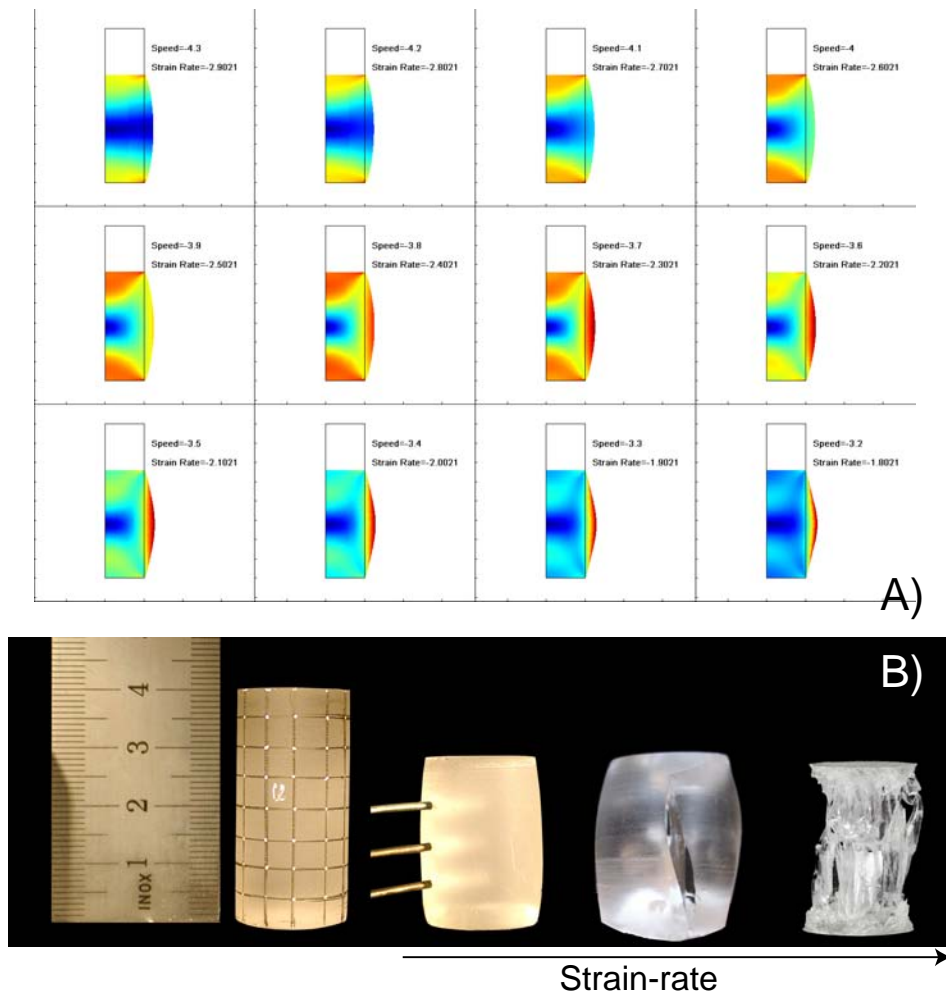
Figure 2.8: A) Temperature gradient of the numerical experiment at 580°C for a strain rate range from the temperature increase onset to the experimental brittle failure.We can observe a redistribution of the temperature gradient espousing the expected inverted Von-Mises map. Moreover the maximum of the temperature gradient corresponds to the observed tensile cracks in the experiments. Such cracks never been observed for lower strain-rates. Above and due to the strain localisation, the shape of the cylindrical surface is modified. At this strain-rate, brittle failure is experimentally observed. B) Corresponding experimental pictures: intial state before low , intermediate and high strain-rates. Note that the interemediate and high strain-rates have been run without thermocouples in.

2.4 Discussion

2.4.1 The boundary effect

Viscous heating is the manifestation of the deformation of a fluid. It is the consequence of a system attempting to reach a lower energy level by relaxing the stress applied. We observed that for constant velocity experiments the heat gained decreased with time when the viscous heating effect becomes efficient. This fully supports the idea of a self destruction of the viscous heating with time. However and thanks to our system where the boundary conditions is evolving with time we observed that this heat gained began increasing when the system cools down. This result suggests two important points: 1) Even if the temperature increase disappear with time, the viscous heating is still there for a while and may have enough time to localise the deformation. As a consequence the viscous heating effect would be here the generator of shear bands that would later drive the deformation. 2) Because the constrain remains there, the material may find an equilibrium where the heat gained remains constant. At this stage, small thermal gradients would remain present. 3) This observation can simply explained why the viscous heating effect is not easily observed on the field.

In any case it appears that the viscous heating is a time dependent process where the heat gained is dependent on the temperature variations of the boundaries.

2.4.2 Viscous heating and the apparent Non-Newtonian effect

Melt in geology can behave in a viscous or elastic way under the same pressure and temperature conditions. The best example of these viscoleastics magmas remains the mantle; approached as a convective fluid from geodynamicians or a compressive solid for seismologist. Thus the same material exhibit either a fluid or solid behaviour depending on its relaxation state. This idea has been well interpret by Dingwell1996 explaining at the same time another important geological transition: the flow or the blow of volcanic systems [*Dingwell and Webb* 1990; *Dingwell* 1996]. It is likely a competition between the undergone strain rate $\dot{\epsilon}$ and the relaxation timescale (τ) that will determine the state of the material.

Maxwell proposed his visco-elastic model in 1867 [*Maxwell* 1866] and defined the structural relaxation timescale as:

$$t_r = \frac{\eta}{G_\infty} \tag{2.8}$$

where η is the shear viscosity and G_∞ the infinite frequency elastic shear moduli (approximated at $10^{10} \pm 0.5$ Pa for silicate melts as referenced in *Dingwell and Webb* [1989]).

It is noteworthy to observe that previous surveys linked this relaxation timescale to the onset of the non-Newtonian behaviour of silicate melts but also their brittle onset [*Webb and Dingwell* 1990b]. It appears that the melt exhibit a stress and strain rate dependant viscosity when it borders a thousand of this relaxation timescale and fails when it reaches an hundred.

We have been comparing these values to the results obtained with the viscous heating (see Fig. 2.9). We can observe that the onset of the non-Newtonian behaviour is in good agreement with the temperature increase onset. We confirm that while approaching the structural relaxation timescale the material self heat up and exhibit a pseudo non-Newtonian behaviour as its viscosity decrease [*Hess et al.* 2008].

The second observation that can be done on this graphic is the intersection between the Brinkman number line of 1 and the hypothetical failure curve. The crossing point appears to be around 530°C. It surprisingly corresponds to our glass transition temperature range measured with three different methods. Technically it means that once the material "freeze" through the glass transition the viscous heating is not efficient any longer.It involves for example that a fluid deforming below this limit would crack before to exhibit any temperature increase linked to the viscous heating. the viscous heating effect occurs as a non-Newtonian effect only above the glass transition.

However, brittle behaviour can also produce shear heating through the friction of the fractures plains. Thus the creep deformation also generate a shear heating.
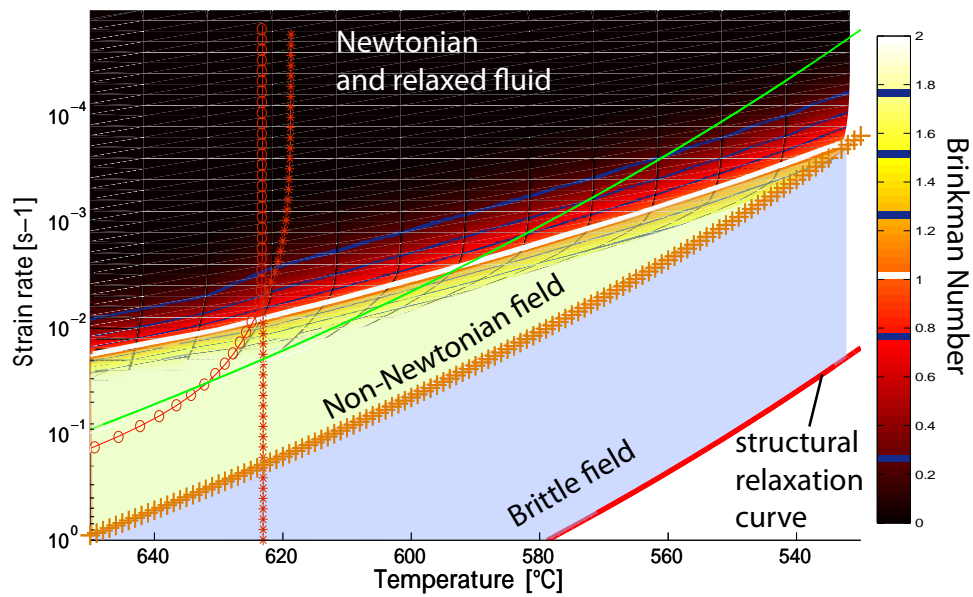
Figure 2.9: A representation of the experimental timescale (proportional of the invert of the strain rate here) against the temperature. We also plot the brinkman number map obtained from our simulations. Finally we represent the structural relaxation time (red line) and the commonly believed brittle onset (orange crosses) and Non-Newtonian onset (green line).
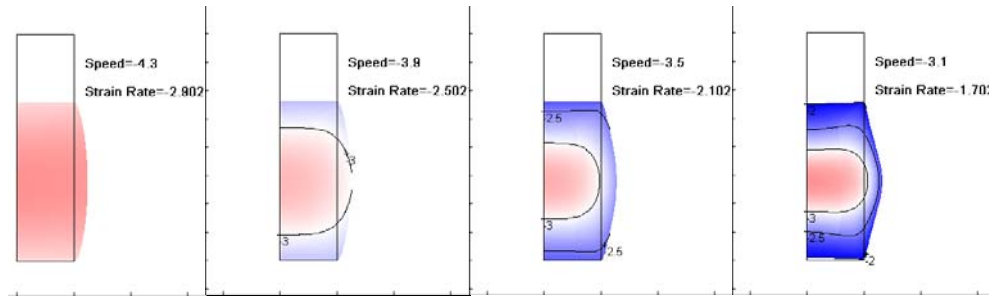
Figure 2.10: Condition.

Here we suggest that most of the non-Newtonian effects observed in silicate glasses and described in the literature may have a strong viscous heating contribution. The effect would be not non-Newtonian any longer but could be described as a thermally unrelaxed fluid. Thus, it changes slightly the previous we had of the silicate fluids. Even if it remains a good approximation the non-Newtonian onset, classicaly describes may be more link to the fluid state and the energy transfered to the system. It concludes that this onset will get more distant of the structural relaxation curve as the temperature increase.

2.4.3 Viscous heating and the brittle onset

theory says that once the stress overcomes yield stress, brittle failure occurs. Following the Maxwell model, Markus *Reiner* [1964] will define a dimensionless number based on this idea: the Deborah number. It represents the ratio between the characteristic relaxation time of the material over the characteristic timescale.

$$De = \frac{t_r}{t_o} \tag{2.9}$$

In other words it defines the "fluidity" of the material; for high deborah numbers the material will act as a solid while it will responds as a fluid for low ones. According to our previous assumptions, the non-Newtonian effect will appear for De=10^{-3} and the brittle onset should occur around De=10^{-2}.

As we saw above the viscous heating is a viscous effect. As a consequence a temperature increase will decrease the viscosity and increase the dynamic of the system, but it will also lower the timescale. Thus the viscous heating will simply shift the system to a more excited state without making it more prone to cross the brittle limit. The viscous heating will theoretically deviate the material to smaller timescale and will delay the appearance of brittle behaviour in the samples (e.g. cracks).

Competitively and depending of the boundary conditions (i.e. stress, velocity and/or temperature), the viscous heating will often create a thermal gradient which will localise and create a weak layer generator of shear bands. More effective is the viscous heating, thinner is the shear band and the active deforming area. In Fig.2.10 we can observe strain rate evolution of the relaxation time. We already observed the link between the thermal gradients and the corresponding cracks. In Fig.2.10 we mapped the Deborah number.The contour gives the logarithmic value of the Deborah number. The colors describe: in red a fluid like behaviour, in white to light blue the transition to a brittle behaviour and in dark blue the value and above of a Deborah number equal to 10^{-2}. It is experimentally admitted as the critical failure value of the sample.

The brittle value reach the sample boundary in the numerical simulation at a strain rate where the failure occurs in the experiments.

2.5 Conclusions

In this survey we show on a small scale the viscous heating effect on cylindrical silicate melts. Here we put the finger on the link between stress, strain rate and temperature effects. The numerical results have been constrained experimentally and have for single degree of freedom, the error linked with the experimental error. The results suggest strongly that most of the non-Newtonian effect observed in silicate glasses is to link to the viscous heating effect. Consequently this non-Newtonian effect is only apparent if corrected for the temperature increase.

Moreover we show here that viscous heating have an important effect on the temperature redistribution within the sample and take a pattern similar to were the cracks later occur (i.e. In a place where, without viscous heating, we would expect a low Von Mises stress, tensile crack are observed).

Even if a theory still need to be elaborated, it involves that the fluid are extremely dependent of the viscous heating efficiency. The non-Newtonian onset and the brittle onset are here observed through a simple energy evaluation.

The range of viscosity investigated here is typical of lava domes. A similar process can consequently be expressed there. An other important point stressed here is that even for constant velocities the viscous heating may have time to initiate thermal and strain gradients before its own 'self destruction'. Consequently and as noticed in *Burg and Schmalholz* [2008] viscous heating may explain the formation of large scales shear zones controlling the formation of orogens even for

constant strain-rate boundary conditions. The viscous heating is thus probably the onset of many geological processes.

2.6   Appendix A: vertical boundary condition

The temperature of pistons is continuously recorded, their temperature is roughly 10 °C lower than the temperature recorded within the sample. Special care has been consequently took in measuring and modelling correctly the atmospheric temperature within the press, lower than the temperature set on the furnace. The temperature profile recall an hyperbolic paraboloid surface (horse saddle). The extremes are the temperature of the furnace and of the piston. The critical point is a variable depending of the distance between the pistons. It reach one or the other extremes depending if the pistons are away or in contact. In between it appears as an error function (T°C vs h) where the inflexion point is around a height equal to the distance from the furnace.

For this survey we approximate that the piston temperature remains the same along the radius of our sample. We will also neglect the temperature variation due to the increase of the radius as the dimension of our sample leave us in the lowest temperature gradient. Finally and because we are with the dimension of our sample and our strain limitation, we noticed that we were in a poorly curved part of the error function; we consequently approximate the temperature decrease due to the piston as a linear function:

$$T_a = -58.63 frac((T_f - T_p) * (-h) - 1.394)2 \qquad (2.10)$$

Finally the temperature profile on the cylindrical surface is described as follow:

$$T_l = T_p + (T_a - T_p) \left[2l \left(\frac{1 - l}{2} \right) \right] \tag{2.11}$$

Where h is the sample height, l is the normative length of the boundary, T_f is the furnace temperature, T_p the piston temperature, T_a the atmospheric temperature

Chapter 3

The non-Newtonian effects of Crystal Bearing melt

"It sure does, Ben, it definitely does...this is definite...it specifically clearly, unequivocally says that Russia and other countries will enter into war and God will destroy Russia through earthquakes, volcanoes..."

Pat Robertson, *when asked the question "Does the Bible specifically tell us what is going to happen in the future".*

This chapter introduces the effects of crystal bearing melts on the rheology. It offers a case study on the Mt. Unzen volcano and its well known 1990-1995 eruption. Transitions between effusive and explosive styles of lava dome eruptions are likely accompanied by changes in lava rheology. The common presence of crystals in dome lavas produces a complex non-Newtonian rheology. Thus models of such complex rheology are essential for volcanic eruption models.

Here, we have measured the rheology of natural Unzen lavas with a compressive uniaxial press operating at stresses between 1 and 70 MPa and temperatures between 940 and 1010°C. Crystal-rich Unzen lavas are characterised by two essential rheological features which produce non-Newtonian effects. The first is an instantaneous response of the apparent viscosity to applied stress which requires that the magma be described as a visco-elastic fluid that exhibits shear-thinning. The second effect takes the form of a time-dependence of the viscosity at moderate to high stress ($\geq$ 10 MPa). In this regime, the apparent viscosity slowly decreases as increasing fracturing of the phenocrysts and the groundmass occurs. Fragmentation of crystals and alignment of crystal fragments are observed to produce flow banding-effects which in turn lower the apparent viscosity of natural dome lavas. Ultimately, deformation may lead to complete rupture of the lava if the stress is sufficient. Cracking thus stands as an important process in natural dome lava rheology. The ubiquitous non-Newtonian rheology of dome lavas, observed experimentally here, needs to be adequately treated in order to generate appropriate eruption models.

3.1 Introduction

Unzen is a back-arc volcano enclosed in the Beppu-Shimabara graben, located on Shimabara peninsula in Kyushu Island, Japan. The most recent activity of Unzen began in November 1990 after 198 years of quiescence. An initial phreato-magmatic eruption was later followed by an explosion in April 1991 and the first lava dome extrusion in May 1991. Over the following five years many cycles of dome growth and collapse occurred as Unzen underwent several transitions in eruptive intensity and style [*Nakada and Motomura* 1999]. Activity ranged from vulcanian explosions to phreato-magmatic eruptions and lava dome extrusions, which culminated in the generation of pyroclastic and debris flows [*Nakada and Motomura* 1999; *Nakada et al.* 1999; *Fujii and Nakada* 1999]. Ultimately, thirteen different domes were created, most destroyed by exogenous or endogenous growth, and activity ending in February 1995. Understanding what drives transitions in eruptive style is critical to volcanic hazard assessment. During the eruptive activity of Unzen two overlaying patterns of activity were apparent: 1) a long-period cycle characterised by two phases 20 months in length, and 2) a short-term cycle in which the eruptive regime alternated between exogenous and endogenous dome growth. The long-period cycles have been attributed to the country rock rheology [*Maeda* 2000]. According to that study the long-period cycles could find their explanation in the elastic properties of the rocks surrounding the volcanic conduit via changes in the volcanic conduit dimension. This idea has been supported by Noguchi and co-authors who developed it in terms of an effusion rate efficiency linked to the crystal content and characteristics (i.e. length, crystal fraction and microlite number density) [*Noguchi et al.* 2007, 2008]. The shorter period cycles have to date been explained by two theories: the self-

sealing model [*Nakada and Motomura* 1999] and the rupture model [*Goto* 1999].
Awareness is increasing that eruptive style transitions may well be driven by the
complex rheology of crystal- and bubble-bearing lavas [*D'Oriano et al.* 2005].
Thus, a better understanding of the lava rheology involved at Unzen (e.g. how
it flows and/or fails) is essential to constrain both the self-sealing and rupture
models.

Suspensions and highly crystalline lavas have complex rheologies, and their
definition is also technically difficult. The addition of rigid particles in a melt
increases its relative viscosity (ratio between the effective viscosity and the vis-
cosity of the solvent). At low crystal fraction, suspensions behave as Newto-
nian fluids (i.e., the stress to strain-rate relationship is linear and passes through
the origin) and their relative viscosity can be approximated by empirical mod-
els such as the Einstein-Roscoe equation [*Roscoe* 1952]. With increasing crystal
fraction, the relative viscosity increase follows a power law [*Eilers* 1941; *Ward
and Whitmore* 1950a,b; *Roscoe* 1952; *Vand* 1948; *Gay et al.* 1969; *Chong et al.*
1971; *Gadalamaria and Acrivos* 1980; *Ryerson et al.* 1988; *Woutersen and Kruif*
1991; *Jones et al.* 1991, 1992; *Lejeune and Richet* 1995]. Numerous attempts
have been made to improve this law but none have achieved widespread applica-
tion [*Mooney* 1951; *Bagnold* 1954; *Krieger and Dougherty* 1959; *Thomas* 1965;
Gay et al. 1969; *Batchelor and Green* 1972; *Jeffrey and Acrivos* 1976; *Batchelor*
1977]. Moreover, at high crystal content, the crystal network effectively hampers
viscous flow once a critical melt fraction is reached and the rheology becomes
strain-rate dependent, i.e. non-Newtonian [*Lejeune and Richet* 1995; *Bruckner
and Deubener* 1997; *Deubener and Bruckner* 1997; *Lavallee et al.* 2007; *Caricchi
et al.* 2007; *Champallier et al.* 2008]. The mechanical heterogeneities generated
by the presence of crystals in a melt allow stress localisation and favour the for-

mation of shear bands causing the premature generation of cracks. The apparent viscosity is then no more homogeneous. It cannot be seen as an effective viscosity in the sense of a phase mixture in continuum but apparent in the sense of acute strain localisation and material failure. This apparent viscosity can be seen as a macroscopic viscous flow that may exhibit discontinuous brittle behaviour on a local scale. It commonly bridges viscous-flow to dislocation-creep behaviour. This has been observed for some time in the structural geology of crystalline rocks [*Nicolas et al.* 1977; *Poirier et al.* 1979; *Poirier* 1980, 1985], polycrystalline flow [*Vandermolen and Paterson* 1979; *Nicolas* 1984; *Shea and Kronenberg* 1992; *Lejeune and Richet* 1995; *Rutter and Neumann* 1995; *Lavallee et al.* 2007], metallurgy [*Jonas et al.* 1976; *Canova et al.* 1980] and even in polymers [*Bowden and Jukes* 1969; *Bowden* 1970]. As a result, measurements of the apparent viscosity of a suspension cannot yet be adequately described. Differentiating each effect of the apparent viscosity decrease is needed in order to create an appropriate model. Here, we study the stress/strain-rate dependence of Unzen lava rheology. In particular we describe the transition from viscous flow to brittle behaviour. Providing evidence that this description is capable of explaining the recurring critical rupture of lava domes during the recent activity of Unzen.

3.2 Methods

We employed a parallel plate geometry generated via a uniaxial press to study the viscosity of natural dome lavas subject to different applied stresses (1-70 MPa) and temperatures (940-1010°C) [*Hess et al.* 2007]. The apparatus is useful for volcanological studies because it can accommodate large samples (up to 100 mm in length and diameter) and it uses conditions equivalent to those found in

deforming lava domes. We used large cylindrical samples (80 mm high by 40 mm in diameter) in order to overcome scaling issues arising from the large size of phenocrysts in Unzen lavas. Samples with an aspect ratio of 2 were chosen in order to meet the classic standards of parallel plate rheometry [*Hawkes and Mellor* 1970]. We inserted three equidistant thermocouples inside the long axis of the sample to continuously monitor the evolution of temperature. The samples were placed between the pistons of the press and heated for seven hours. The upper piston was then lowered until contact with the upper part of the sample was made and this position was maintained for one hour in order to reach perfect thermal equilibrium between piston and sample. Various loads were then applied and the load and displacement were recorded at a rate of 10 measurements per second. The apparent viscosity was calculated from the measured rate of change of the sample's length using Gent's equation [*Gent* 1960; *Hess et al.* 2007]:

$$\eta_a = \frac{2\pi F h^5}{3V \frac{dh}{dt}(2\pi h^3 + V)} \tag{3.1}$$

Where η_a is the apparent viscosity, F is the force, h the length between the two pistons and V the volume of the sample.

As the viscosity of silicate melts is strongly dependent on their chemical composition. Hence, we determined the chemical composition of the interstitial melt in order to understand the apparent viscosity increase caused by the presence of crystals. The chemistry was determined with a CAMECA SX50 electron microprobe. A careful calibration of the instrument was done before each measurement and special care was taken to minimise sodium loss. We used a current of 5 nA, a voltage of 20 kV and a 20-micron diameter beam. The eruptive products of

Unzen are andesitic and part of the calc-alkaline series. The interstitial glass phase, however, is rhyolitic [*Nakada and Motomura* 1999]. Here we studied lava dome samples from 2000 and 2001 fieldwork conducted on different block-and-ash flows deposit. In this study we used samples with low open porosity; namely Muz2000A, Muz2001A and Muz2001B with an open porosity of 3.87, 6.74 and 5.7%, respectively. We also emphasise that the glass matrix has an Agpaiitic index below one (see Table 1). Chemical variations have consequently a small effect on the viscosity [*Dingwell et al.* 1998; *Hess et al.* 2001]. Our work is in agreement with previous rheological studies of Unzen's interstitial melt phase (e.g. [*Nakada and Motomura* 1999; *Goto* 1999]). The recent eruptive products of Unzen volcano are andesitic containing 0.1% to 0.2% volatiles for the dome (lobe 1-13) and 0.4% for the spine (final stage of the eruption)[*Nakada and Motomura* 1999; *Kusakabe et al.* 1999; *Noguchi et al.* 2007, 2008]. The lava erupted at around 780-880°C [*Nakada et al.* 1999; *Holtz et al.* 2005] and originated from the mixing of a hot, aphyric, dioritic magma with a cold, crystallised, granitic magma. Petrographic analyses suggest that the phenocrysts originally from the granitic magma were entrained by the ascending dioritic magma. The phenocrysts total fraction, approximately 30%,is mainly composed of plagioclase or hornblende, with a lesser amounts of quartz, biotite and magnetite. Phenocrysts are often clustered (Nakada and Motomura,1999 and figure 3.1 -A). Plagioclase phenocrysts were often partially fractured (figure 3.1 -B). The groundmass is partially crystallised with 40 +/- 10 volume % of microlites of plagioclase and some pyroxenes and biotite. An important fraction of the microlites appears to be fragments of broken phenocrysts, possibly produced during ascent in the conduit.

	This study- Weight % (average of 11 measurements)	Mean deviation	Nakada- Weight % (average of 7 measurements)	Mean deviation
SiO$_2$	78.34	0.23	77.60	1.41
TiO$_2$	0.43	0.03	0.32	0.07
Al$_2$O$_3$	11.88	0.18	11.21	0.43
FeO*	0.84	0.09	0.94	0.20
MnO	0.03	0.02	0.04	0.03
MgO	0.09	0.01	0.11	0.07
CaO	0.49	0.17	0.63	0.21
Na$_2$O	3.06	0.08	2.95	0.19
K$_2$O	4.79	0.13	4.70	0.37
P2O5	0.02	0.02	X	x
Total	99.97	0.11	98.50	0.96
AgI	0.86	0.02	0.88	0.04

Table 3.1: Chemical composition of Unzen glass determined by electron microprobe (left), and from Nakada (right; 1999). FeO* is the total iron measured. The Agpaiitic index (i.e. $AgI = \frac{Na_2O + K_2O}{Al_2O_3}$) indicates a minor viscosity dependence on the chemical composition variations.
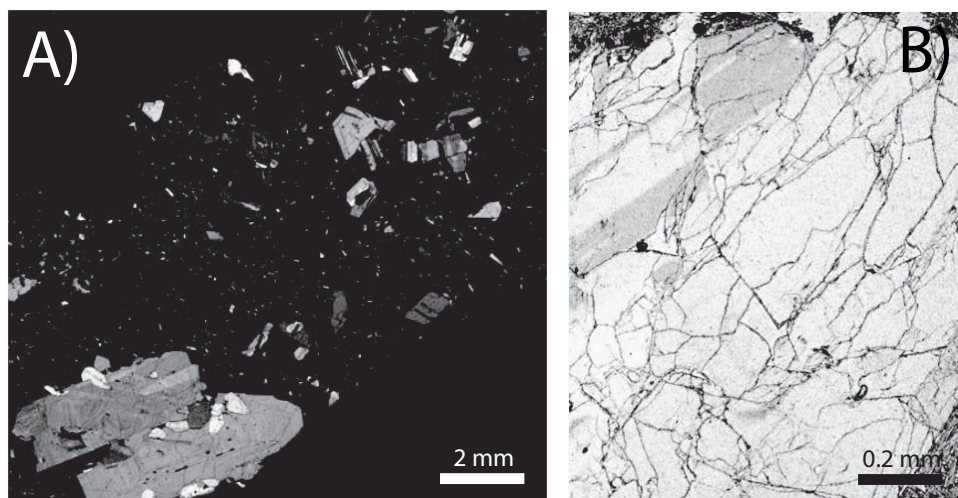
Figure 3.1: Thin sections of the original products of Unzen. (A) is a crossed polarized light view of the clustered phenocrysts, embedded in a glassy groundmass containing crystal fragments and intact microlites. (B) A highly fracture plagioclase, typically found in Unzen.

We estimated the crystal and vesicle fractions of the samples by automated optical counting. This technique can be reliably used to characterise Unzen samples because the crystal assemblage is simple and distinct. Our method is based on colour coding of scanned images. The ratios between red, green and blue colours help distinguish between crystal types. The fingerprint of each crystal can thus be used to determine and patch the surfaces of all the crystals of that type. Each patch is then numbered and oriented, and thus the number of crystals, their surface fraction and the anisotropy can be estimated. This technique resolved estimates of 18.16% of plagioclase crystals and 9.10% of hornblende crystals; for a total amount of 27.28% phenocrysts. These are results in accordance with previous studies [*Nakada and Motomura* 1999; *Noguchi et al.* 2007, 2008]). In addition, the samples used in this study contain ≈30% microlites and 5-7% pores. The Unzen lavas used in this study contain approximately 45-60% crystals and their deformation is therefore expected to be strain-rate dependent at eruptive temperatures.

3.3   Results

3.3.1   Viscosity measurements on natural samples from Unzen.

More than 20 experiments were performed under different temperatures and applied stresses. For a given stress the value of the apparent viscosity recorded is characterised by a shear-thinning (figure 3.2). At the lowest applied stress of 2.8 MPa the apparent viscosity increases until it stabilises to a constant value. The lowest stress deformation experiment provides an approximation of the near

static viscosity of the suspension (i.e., the apparent viscosity corresponding to an infinitesimally small stress).

At higher applied stresses an unexpected time-weakening effect starts to cause a decrease in the viscosity (figure 3.2). At even higher stresses, the apparent viscosity decreases further. A minor amount of heating (up to 3°C) is produced by viscous dissipation and sample failure occurs as the system reaches the brittle regime (see dashed line in figure 3.2). We have, consequently, two rheological effects: 1) an instantaneous shear-thinning, and 2) a weakening effect evolving with time.
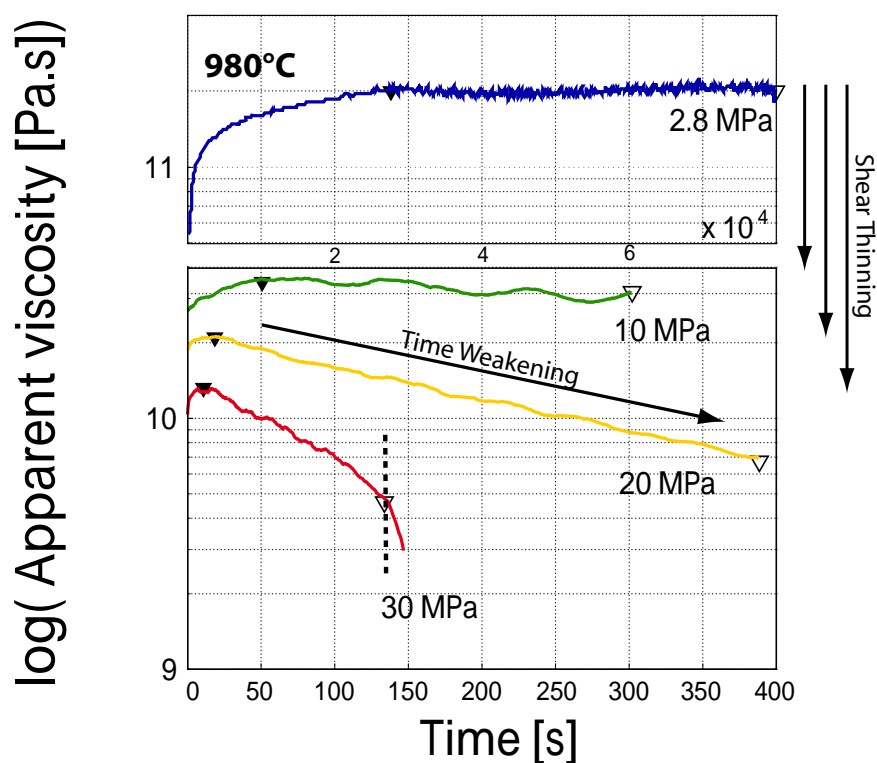
Figure 3.2: Apparent viscosities measured during experiments at 980°C under applied stresses of 2.8, 10, 20 and 30 MPa, respectively. The vertical arrows highlight the instantaneous viscosity decrease (shear-thinning effect) accompanied by each stress increment. At low applied stress, the viscosity remains high and constant, but with increasing applied stress the viscosity becomes time dependent and displays a delayed decrease (time-weakening effect). At the highest stress rupture of the sample occurred (dash line). Triangles show the initial (filled symbols) and final values (open symbols) considered in the rest of this study.

As with any suspensions containing rigid particles, the bulk fluid can be assumed to be viscoelastic and described as a Jeffrey-like model or Burgers model if the solvent is assumed to be viscoelastic itself [*Strivens* 1983; *Jones et al.* 1991; *Bagdassarov et al.* 1994]. As a consequence such systems exhibit two relaxation times, the first one is the relaxation time of the liquid that can be described for silicate melts with a classic Maxwell model [*Webb and Dingwell* 1995] and range between 0.05 and 1 second in our experiments. The second one is a delayed relaxation time linked to the particles; the bulk elastic modulus (but also the yield stress) being dependent on the crystal fraction. Once those two relaxation times are exceeded the suspension behaves as a fluid.

Due to the above, we decided to use the onset of the relaxed linear viscosity as our initial value, as this best represents a fluid-like state. It is also the most relevant value for volcanic timescales, as already discussed by Sparks and co-authors [*Sparks et al.* 2000]. If the linear regime is not reached, the apparent viscosity peak is chosen as the most relevant and closest value of the relaxed state.

The applied stress proportionally affects the shear-thinning effect on a logarithmic scale ([*Lejeune and Richet* 1995; *Lavallee et al.* 2007]; see figure 3.3). We can observe a viscosity-stress relationship which in turn is dependent on the temperature of the suspension. Moreover, the time-weakening effect serves to further decrease the viscosity and it appears to increase with applied stress. In our experiments its onset is in the range of 10^7 Pa. The amount of decrease was however limited as the maximum applied strain was restricted to 25% total strain.
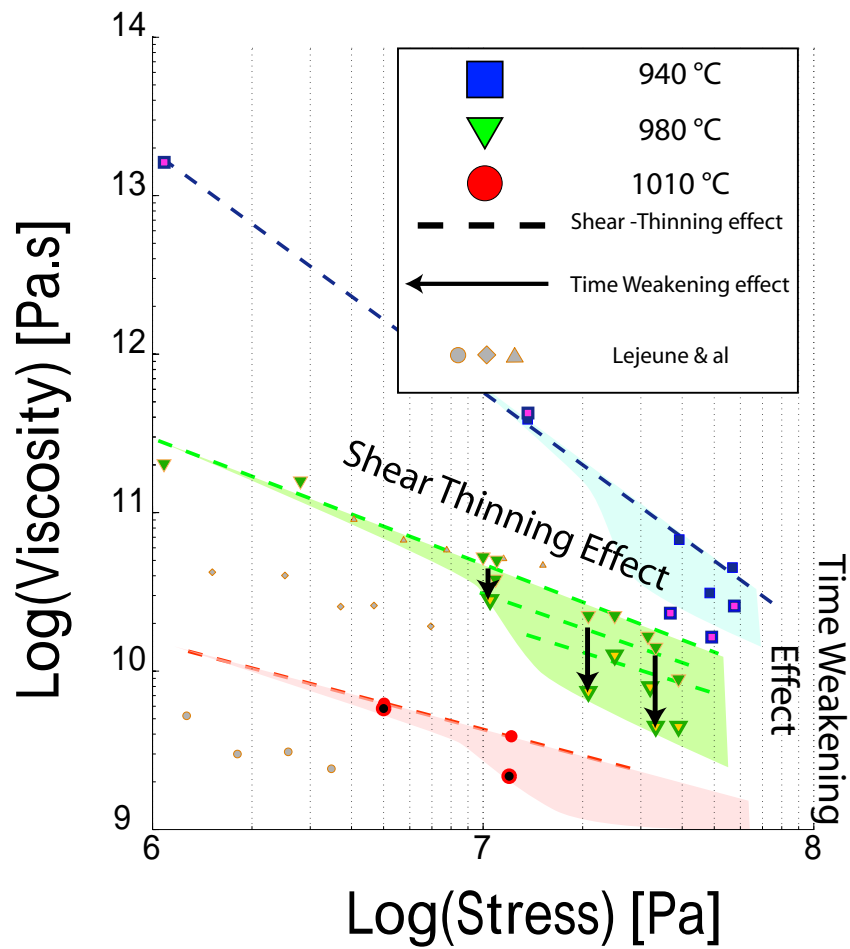
Figure 3.3: Apparent viscosity against stress. Filled symbols represent the initial measured viscosity while the unfilled symbols represent the end value. The shadows highlight the potential impact of the time-weakening effect; its onset being around 10^7 Pa in our experiments.(N.B: For low stresses, initial and end values are superimposed)

3.3.2   Characterisation of the shear-thinning

Recovery experiments were performed to characterise the shear-thinning. To this end, we applied a pressure of 10 MPa and maintained it until the viscosity became constant. Then a load of 30 MPa was applied, maintained for approximately 200 seconds, and then released to 10 MPa (see figure 3.4). Upon loading to 30 MPa an instantaneous viscosity decrease of approximately 0.3 log Pa.s is measured which is instantaneously largely recovered when the stress is released back to 10 MPa (the residual being below the apparatus error). All that remains after unloading is the viscosity difference between both runs at 10 MPa which corresponds to the non-recoverable viscosity decrease (time-weakening) recorded during the 30 MPa run.
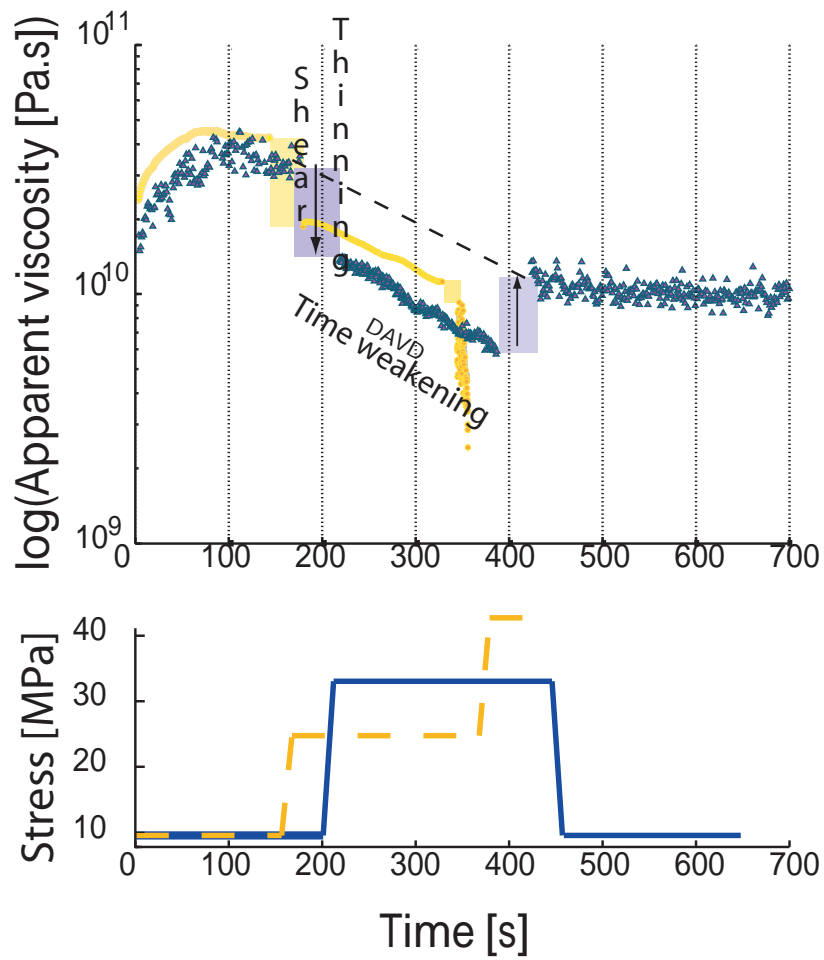
Figure 3.4: Multi-stress experiments. Example of instantaneous apparent viscosity profile obtained during a recovery experiment in which 10, 30 and 10 MPa were successively applied.

3.3.3 Characterisation of the time-weakening effect

Experiments were performed to characterise the time-weakening in lava deformation within the brittle field. This allows us to observe how the sample passes through the brittle-ductile transition. In these experiments, we observe a decrease in viscosity punctuated by small jolts (see domain A in figure 3.5). These jolts result from cracks which we can monitor acoustically; as the stress is held constant, any crack will accelerate the piston and give a strain-rate jolt. Transitional domain B records a change in the time-weakening rate (e.g. slope of viscosity versus time). In this domain cracks are easily acoustically recognised (this brittle phenomenon is confirmed by a more 'noisy' curve). For case I (i.e., between 20 and ≈30 MPa) the rate decreases and the viscosity approaches near-constant values. In contrast, in case II (i.e. above 33 MPa) the rate of viscosity reduction increases and generally leads to a final failure in domain C.
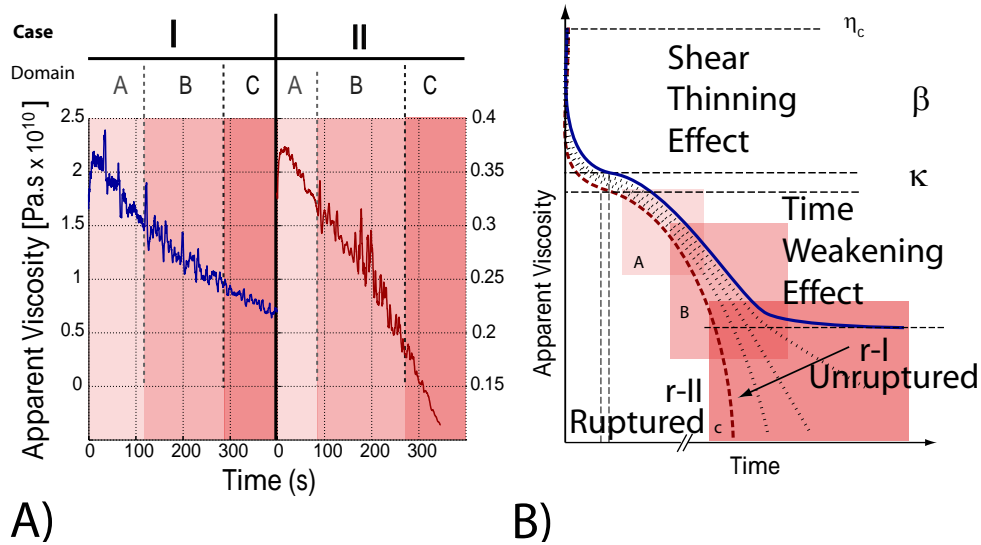
Figure 3.5: A)Viscosity-time evolution for a non-ruptured (I) and ruptured sample (II). Stresses applied are respectively 21 and 39 MPa; both experiments were performed at 980°C. B) Summary sketch of the different processes observed: Starting from its static viscosity η_c, a shear-thinning effect is followed by a time-weakening effect which can lead to complete failure, if a stress limit is crossed. The final stage (c) can be already predicted with the domain (b) according to the sign of the second derivative of this domain. (N.B. In this sketch the relaxation time of the melt has been simplified).

3.3.4 Post-experimental textures and structures

The deformation experiments performed in this study help explain some of the textures and structures observed in Unzen's volcanic products. Post-experimental analyses show a crack distribution more or less parallel to the maximum stress field, as expected for deformation of a homogeneous cylinder in compression. The crystals appear to influence where cracks grow and in some cases apparently strong, intact crystals appear to deflect locally growing cracks. At high stresses, cracks propagated across the crystals and shear zones developed in which crystals were completely crushed and pulverised to powder. Plagioclase phenocrysts were especially susceptible to such crushing and the crystals which were most extensively pulverised were not preserved during thin section preparation. For such cases, voids of the former crystal shape are observed often with some residual fragments on the edges. This process confirms observations made on natural systems. Phenocrysts embedded in eruptive volcanic products commonly appear in a fragmented form. As mentioned by Allen & McPhie [*Allen and McPhie* 2003], such fragments are commonly observed in explosive systems [*Branney et al.* 1992; *Best and Christiansen* 1997], but rarely in effusive ones [*Allen* 1988]. Transitional regimes such as volcanic domes most commonly contain crystal fragments.

However, their study is hampered by the necessity of reassembling fragments more or less isolated by substantial strain. Nevertheless, their extent of fragmentation does not appear to be a function of the distance from the vent or the transport process [*Allen and McPhie* 2003]. Therefore it is thought that crystals are cracking in response to differential stress changes inside the volcanic conduit rather than during aerial transport [*Kennedy et al.* 2005]. This also correlates with the fact that volcanoes are likely to undergo high shear stresses on the upper conduit margins, a domain where brittle behaviour is commonly inferred [*Tuffen*

and Dingwell 2005]. Phenocrysts seem to be generally broken by a rapid decompression of the magma and to a lesser extent by transport processes such as a pyroclastic flow [*Fisher and Schmincke* 1984].

Different processes may explain the formation of crystal fragments: (a) vacancies and matter diffusion; (b) dislocation of frank network and slip; (c) grain boundaries and joints [*Poirier* 1985]; (d) melt inclusions [*Allen and McPhie* 2003]. Additionally, all crystals do not react in the same manner. Plagioclase crystals are commonly more sensitive to stress, while hornblende but especially quartz and pyroxene are less prone to fracture. In our experiments, dislocation is the most commonly observed process, plagioclase being more affected than hornblende.
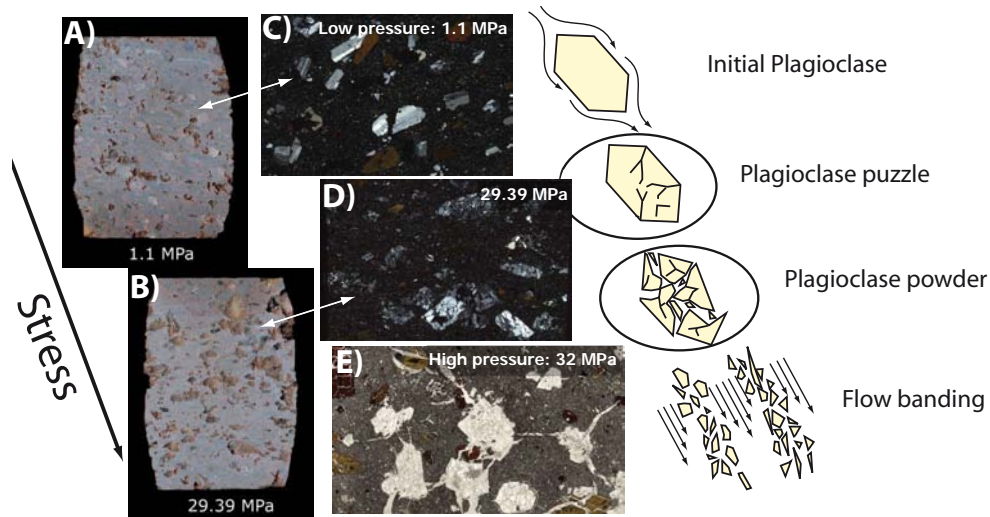
Figure 3.6: (A) & (B) are cross-sections of the samples for different pressure at 980°C and 25% of strain. Both exhibit holes previously holding phenocrysts reduced to powder by the deformation; however, low pressure experiments are showing most of the phenocrysts still in position while most of them are crushed and removed for high pressure experiments. (C),(D) & (E) are microscopic observation after deformation. (C) low pressure experiment exhibiting more cracked phenocrysts ("crystal puzzle") and phenocrysts fragments of type 2 according to the Allen & McPhie classification. At higher pressure experiments, (D), phenocrysts start to dislocate and their fragments are reduced to smaller sizes. The last stage, (E), exhibits powder of plagioclase that was not always preserved during thin section preparation ("crystal ghost"). In contrast to the other two, this last picture is simply under plane polarised light in order to offer a better view of the cracks; commonly observed at this stage. The cartoon on the right hand side summarises the plagioclase phenocryst fragmentation to an ultimate stage of flow banding.

Allen & McPhie classified plagioclase fragments in 5 categories [*Allen and McPhie* 2003]. Our observations in thin section appear interpretable within that context. In a regime of low stress experiments, plagioclase exhibit pronounced cracks and may exhibits simple breakage into two parts, e.g. type 2 of Allen & McPhie (see figure 3.6-C). At higher stress, the size of plagioclases is reduced to fragments and yields a "plagioclase puzzle", e.g. type 3 of Allen & McPhie classification (see figure 3.6-D). Further decrease of the grain size yields the appearance of crystals losing their recognisable shapes similar to type 4 of the above classification. At the highest stresses, we obtain plagioclase powder which is lost during thin section preparation (see figure 3.6-E). We name such holes "crystal ghosts" and these may indeed correspond to the extremely fractured crystals observed as type 5. To summarise, it appears that the classification type 2 to 5 of Allen & McPhie can be successively generated in our experiments by increasing stress.

Our observations suggest that the fragmentation of crystals upon shearing enhances the formation of shear bands. By focusing the stress on the tips of crystals fracturing occurs. This generates a trail of broken crystals as documented in silicic lava [*Tuffen et al.* 2003; *Tuffen and Dingwell* 2005]. Such a phenomenon may be an explanation for a characteristic flow banding in the products of volcanic conduits [*Gonnermann and Manga* 2005].

3.4 Discussion and comparison of rheological results.

3.4.1 comparison of rheological results

In order to generalise our results, we compare them below to recent studies [*Lejeune and Richet* 1995; *Caricchi et al.* 2007; *Champallier et al.* 2008], see figure 3.7-A. Such a comparison between different products needs to be based on the relative viscosity in order to extract the physical influence of cristallinity. Comparison leads to the following general observations: 1) All studies show a stress-dependent relative viscosity (identified in our study as shear-thinning). 2) All studies indicate that this dependence is a function of the crystal fraction. 3) Most of the experimental data exhibit a linear relation between the relative viscosity and the stress. This last point will be critically challenged later in the discussion, but assumed to be valid in this section.

A)

B)
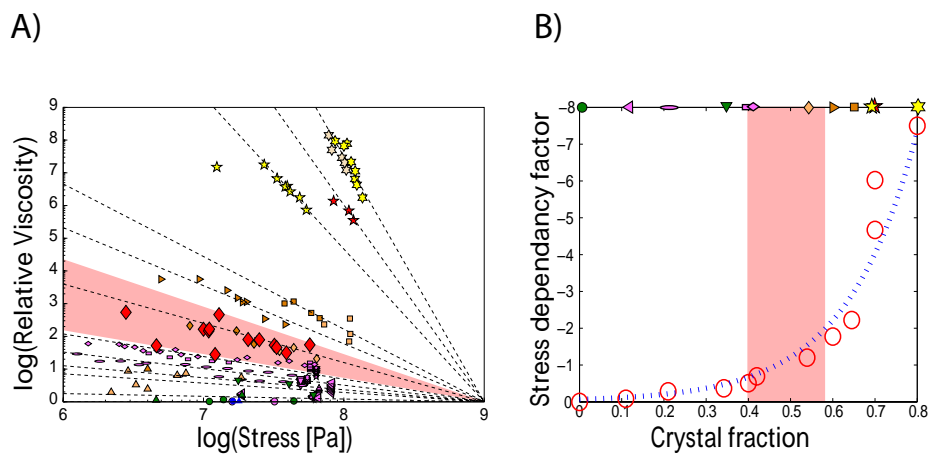
Figure 3.7: (A)Relative viscosity vs. stress, computation of recent studies with the present survey (see the text). Each symbol is a different crystal fraction annotated on the right hand side graphic. The shaded area is the range of Unzen data (diamonds). It fits with the crystal fraction measurements observed for Unzen. (B) Stress dependency factor (slope of the first graphic) is related to the crystal fraction via $-(0.06exp(6*\phi))$.

A linear relation can be approached by an Ostwald-De Waele power law [*Ostwald* 1925] modified according to the following 2 points: A) it is commonly observed that this viscosity decrease corresponds to a transition between two Newtonian apparent viscosities. The results of Jones and co-workers on suspensions have shown a tendency to reach a limiting stress value independent of the initial crystal fraction [*Jones et al.* 1991, 1992]; observations on olivine for different crystal sizes have shown the same tendency [*Frost and Ashby* 1982]. B) Moreover the work of Caricci and co-workers suggests that the final configIIIuration of crystal-bearing melts would be a crystal alignment offering magmatic channels for the melt [*Caricchi et al.* 2007]. This observation, confirmed in this study, recalls the percolation of a system fitting to Darcy approximation for a Poiseuille Newtonian flow (i.e. $\vec{\nabla}\sigma = \eta \frac{8L}{D^2(1-\phi)} * \dot{\varepsilon}$ where L is the length of the channels and D their diameter). Thus the effective viscosity of a fluid with such configIIIuration will be equal to the melt viscosity within a geometric factor.

In a first approach we thus allow the second Newtonian regime to be reached for a stress limit and fitting to a relative viscosity of 1. In our experiments we observe that the relative viscosity of 1 will be reached for a critical stress of 1 GPa. Starting from this hypothesis and fitting each experiment, we can find the stress dependence factor of the viscosity drop for each crystal fraction (see figure 3.7 part B). This yields the following relation for the stress dependence of the relative viscosity of crystal-bearing melts:

$$log(\eta_r) = (-0.06exp(6 * \phi)) * log\left(\frac{\sigma}{\sigma_{lv}}\right) \qquad (3.2)$$

where η_r is the relative viscosity, σ is the differential stress, σ_{crit} is the limiting

stress value (here $10^9 Pa$), and ($0.06exp(6 * \phi)$) is the crystal stress dependency relation with ϕ the crystal fraction.

It may be worth noting the similarity of the curves between this shear-thinning dependence factor and the static relative viscosity as a function of the crystal fraction. The effect of crystals on the static relative viscosity seems here to be balanced by the stress. This notion has already been partly observed by Champallier and co-workers (2007) who noticed a different slope of the flowing curve (e.g. stress versus strain-rate) for each crystal fraction. The stress limit point may vary slightly according to the crystal fraction, especially for low crystal content. Moreover the time-weakening effect is not taken into account in this model; even if observed by Champallier and co-workers, its magnitude appears to be a function of the confining pressure. However, these effects cannot yet be constrained and will require further investigation.

Although this model does not aim to be quantitative, it nevertheless offers a physical explanation of the viscosity decrease in agreement with previous literature. Moreover, using this model for Unzen data, we predict a crystal fraction in agreement with the measurements (see figure 3.7 part B).

3.4.2   Discussion

As mentioned earlier, magmas can be understood as visco-elastic fluids. Their behaviour is dependent on temperature [*Griggs et al.* 1960; *Murrell and Chakravarty* 1973] and confining pressure [*Paterson* 1958; *Rummel and Fairhurst* 1970; *Karato et al.* 1986]. Those two parameters make the system fluid and delay the appearance of cracks by dissipating most of the energy added to the system. High crystal fractions are hampering this dissipation. Adding elastic particles able to form networks makes the whole system less viscous and consequently less prone to

dissipate the stress [*Lejeune and Richet* 1995]. It leads to a premature generation of cracks and shifts the system response into the brittle field. Our experiments distinguish between effects which control the apparent viscosity of natural samples with applied stress increments.

The first observed decrease of viscosity with applied stress is characteristic of shear-thinning. Unloading experiments (see figure 3.8) have shown that this effect cannot be a viscous process and has to be predominantly elastic and/or brittle. During complementary experiments on synthetic crystalline sphere-bearing melts, Lejeune and Richet (1995) observed a very similar dependence of the viscosity on applied stress (see figure 3.7). This effect seems to be independent of the confining pressure as confirmed by the similarities between the studies of Champallier et al. 2008 and Caricci et al. 2007 (both under confining pressure) and Lejeune et al. 1995 and this study (atmospheric pressure). It favours an elastic origin rather than a brittle one. Moreover, the melt viscosity is therefore independent of the applied stress at this temperature. Even if viscous heating may have a contribution, it does not appear to explain such a viscosity decrease [*Hess et al.* 2008].

Here, we attribute the shear-thinning effect to the presence of crystals in lavas. The crystal fraction will respond first to the stress applied. Elastic compression of crystals will open new channels that initiate an anisotropy in the melt and decrease the apparent viscosity. However, this elastic effect finds its limit in the brittleness of the crystals. Two orders of magnitude before the limiting stress value (σ_{lv}) crystals will start to align and crack. This represents the onset of the time-weakening effect (σ_c) here fixed around 10MPa. The time-weakening effect will stack to this shear thinning, generator of flow banding, it will accentuate this

anisotropy and lead to the limiting configIIIuration suggested by Caricci et al. (2007). This process has also been observed by Lavallée and co-workers (2008).
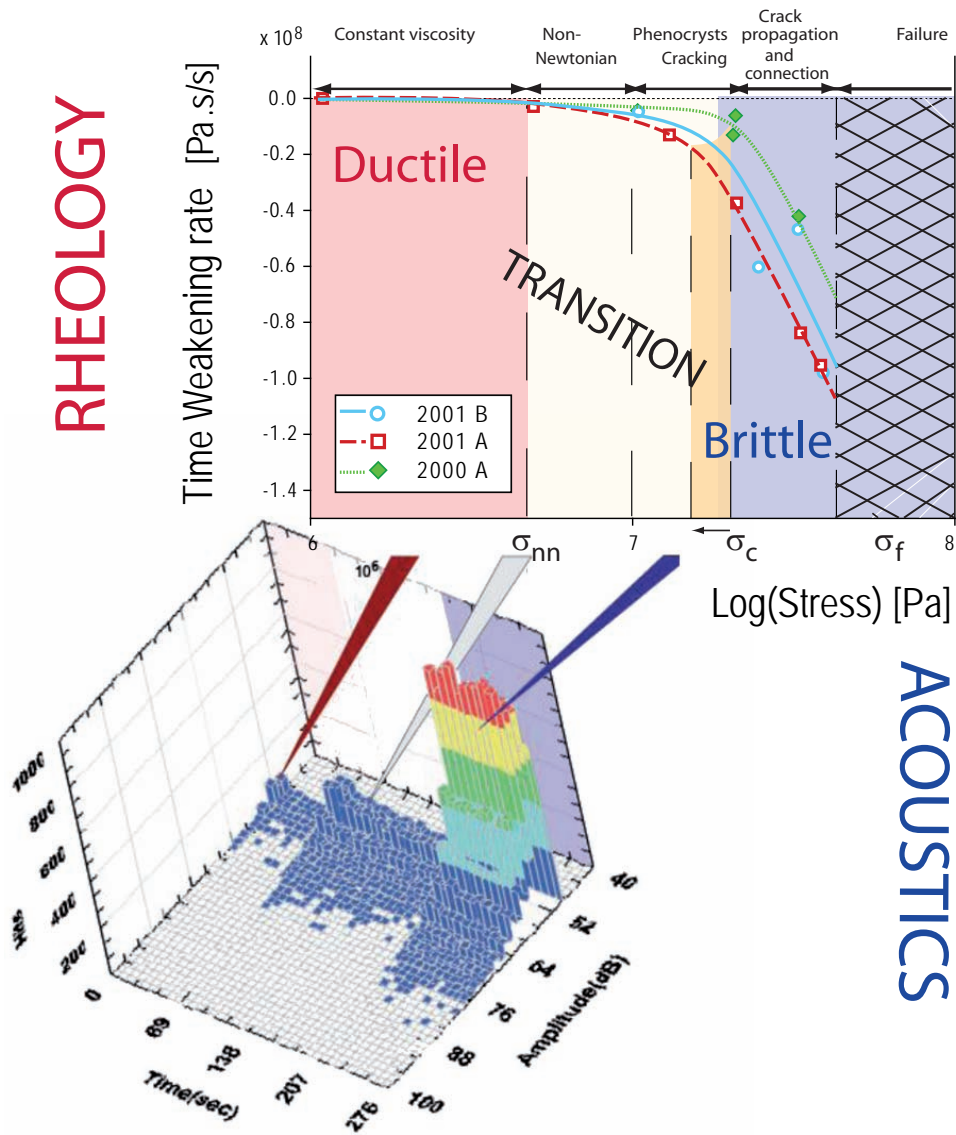
Figure 3.8: Viscosity variation rate in the time-weakening regime according to applied stress. σ_{nn} is the onset of the time-weakening domain; σ_c is the onset of the brittle domain where the cracking most affects the changes in viscosity; σ_f provides the upper limit for the complete failure of the sample when macroscopic cracking prevails. (N.B: due to a different order of magnitude the time-weakening rate of failure experiments is not presented)

The onset of the time dependence of the viscosity of multiphase lavas (referred to as time-weakening effect) was observed to be gradual. Whereas at very low applied stress (1-3 MPa) the viscosity remained constant through a measurement, an increasingly stronger decrease of the viscosity through time was observed for higher applied stresses (see figure 3.8). Between 3 and 10 MPa, no evidence of cracks was observed and we believe that the decrease of the apparent viscosity is due to a structural organization of the groundmass such as crystal alignment and rotation (non-Newtonian field in figure 3.8). Above this value, as also reported in previous studies [*Lavallee et al.* 2008] the cracking of large phenocrysts and the alignment of the fragments produces flow banding structures which ease the flow of the suspension and lower the viscosity. This onset of 10^7Pa is in complete agreement with the shear strength of natural lavas [*Voight et al.* 1999; *Gonnermann and Manga* 2003; *Tuffen et al.* 2003; *Neuberg et al.* 2006]. However, shear strength may vary with the bubble content and the porosity (increasing or decreasing according to the capillary number value); indeed we can observe in our experiments an earlier time-weakening onset for material with higher porosity (see figure 3.8). This observation is in agreement with the observations of Romano and coworkers who claimed a shear strength value of 10^6Pa for pumice [*Romano et al.* 1996]. In addition, we note that this shear strength is comparable to the fragmentation threshold observed by Spieler, Kueppers and coworkers [*Spieler et al.* 2004; *Kueppers et al.* 2006]. We suggest that phenocryst fracture and the time-weakening onset are strongly affected by the porosity.

It appears that magma behaves as a classic visco-elastic fluid. The crystal fraction modifies the macroscopic viscous and elastic moduli of the melt which in turn changes the structural relaxation time of the material. Once the material approaches this relaxation time it becomes brittle [*Dingwell and Webb* 1990;

Dingwell 1996]. The presence of crystals inside magma does not alter this definition; however, it challenges our view of magma rheology at active volcanic systems by modifying the ratio between viscous and elastic parameters.

The time-weakening effect is a destructive process at high stresses and its effect can irrevocably alter the evolution of the shear thinning. The occurrence of cracked crystals weakens and alters the visco-elasticity of lavas in the ductile-brittle transition. Ultimately, complete failure may occur if the stress is sufficient to propagate macroscopic cracks through the melt and crystal mixture.

3.5   Application to Unzen

The melt phase of Unzen lavas has been studied by fiber elongation ([*Goto* 1999]; see figure 3.9). In comparison, our data points at a given temperature show the increase of the apparent viscosity due to the crystal fraction. The maximum increase of apparent viscosity can be encountered for deformation at the lowest strain-rate possible (i.e., under near static conditions). Yet, magmas are visco-elastic bodies with an apparent viscosity which thins upon strain-rate increase. On figure 3.9 this thinning is displayed as the decrease in viscosity; in extreme high-strain-rate cases, we can see that the apparent viscosity nearly recovers the value of the melt viscosity. However, the work of [*Fukui et al.* 1991; *Suto et al.* 1993] claims that the apparent viscosity of Unzen dome was much lower. By considering the water content which may decrease the viscosity [*Hess and Dingwell* 1996], we need 0.13 to 0.55% to correlate the viscosities observed on Unzen volcano. Measurements from Nakada and Motomura (1999) reveal a water content in the groundmasss glass of ≈ 0.2 wt.%. Thus, a good correlation between our measurements, observations and Hess and Dingwell (1996) model is observed.
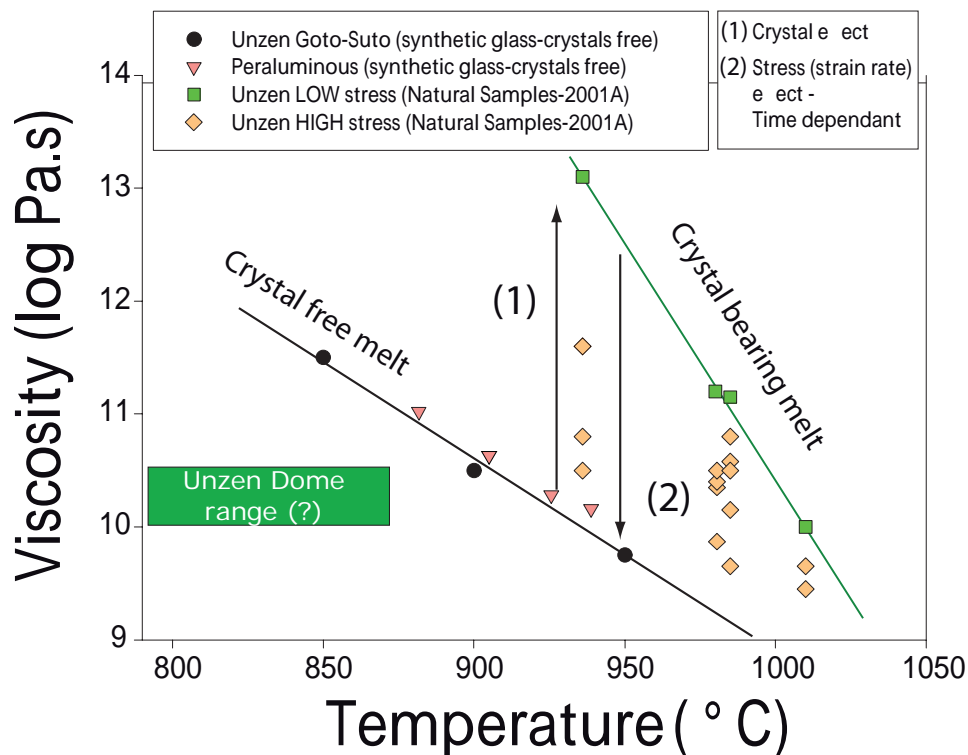
Figure 3.9: Apparent viscosity of Unzen lavas as a function of temperature. Viscosity of the melt was measured by Goto (1999). The results are in agreement with our measurements made on the synthetic, analogue melt HPG8 [*Dingwell et al.* 1998]. The lowest stress experiments provide the zero shear apparent viscosities and therefore show the maximum effect of the crystal fraction. Using the Einstein-Roscoe equation and Unzen's crystal fraction of 0.56, a maximum packing fraction of 0.7 would be required to adequately approximate the observed viscosity increase. Lower estimates of viscosity of Unzen's lava dome as a whole are also presented (i.e. grey box; based on observation during eruption [*Fukui et al.* 1991; *Suto et al.* 1993]). If accurate, these lower estimates would likely reflect a high volatile content or porosity of the lavas present in the dome.

The onset of the ductile-brittle transition of Unzen lavas occurs at moderate differential stresses ($\approx$10 MPa) and ends with the complete rupture of magma around 33-40 MPa. This compressive value is in reasonable correlation with the decompression threshold of 25-30 MPa obtained during fragmentation [*Spieler et al.* 2004; *Kueppers et al.* 2006] at comparable porosities. According to this work, the discrepancy observed between our results and the apparent viscosity measured on Unzen could find an additional explanation. Indeed the dome may evolve through gouge faults eased by a localized higher porosity. This gouge faults evolution has recently been suggested [*Tuffen et al.* 2008]. In this pressure regime melt and crystals fragment independently; specifically, crystals begin to fragment at stress and strain-rates lower than those needed for failure of the pure melt. The premature occurrence of crystal fracturing favours the generation of shear banding which is commonly observed in regions of high strain-rates at the volcanic conduit margins [*Tuffen and Dingwell* 2005; *Neuberg et al.* 2006].

Textural observation of shear banding, in the absence of complete melt fracturing, may thus be used to constrain the moderate stress conditions present inside the volcanic system. It is an indicator of the occurrence of shear-thinning of the magma and thus of a reduced apparent viscosity. Nevertheless, it is important to point out that such a structure may be completely different without a weak crystal phase such as plagioclase or an higher porosity.

This study suggests that eruptions of crystal-rich magmas such as Unzen recent dome growth phases are especially prone to developing shear and brittle textures. Shearing and fracturing are presented here as critical processes that control the rheology of magma and the dynamic of eruptions, and therefore must be considered in all volcanic eruption models. Especially, this improvement of our understanding of magma rheology needs to be incorporated into numerical mod-

els focussing on the volcanic upper conduit and dome in order to not overestimate the apparent viscosity [*Neuberg et al.* 2006; *Costa et al.* 2007; *Hale and Muhlhaus* 2007]. Once fracturing begins, the rheology of ascending magma becomes increasingly dictated by fracturing (unless the deviatoric stress is significantly reduced to the point where healing could occur by closing the cracks) [*Tuffen and Dingwell* 2005]. Strain-rates capable of fracturing magma along the conduit margin would favor the transition from exogenous to endogenous style lava dome growth as observed at Unzen. This thus supports the view that self-sealing of Unzen's endogenous lava dome would bring the lava towards the brittle regime and that further shearing could cause rupture of the plug and exogeneous growth, or formation of a spine. The common occurrence of fracturing of lavas under such extreme conditions would easily lead to the generation of dome collapses and pyroclastic flows. Here we thus postulate that the mere presence of substantial crystal content in magma increases the hazard potential at active volcanoes.

3.6   Conclusions

Here we studied and characterised the rheology of natural lava from Unzen and characterise the effect of the crystal fraction. For the crystal fraction found at Unzen approximation of the apparent viscosity with the Einstein-Roscoe equation may be adequate only under near static conditions (zero-shear viscosity). This work describes two types of non-Newtonian behaviour that may dominate lava emplacement dynamics. The first one is an instantaneous viscosity decrease which shows natural lavas to be visco-elastic fluids exhibiting shear-thinning. The second effect is a time dependent viscosity which becomes more pronounced as the applied stress increases above approximately 10 MPa. In this second regime,

phenocrysts fragment and produce flow banding textures upon further shearing. This regime has a rheology mainly driven by micro-cracking. At even higher stresses (near 33-40 MPa) complete failure of lavas occurs. Our findings support the interpretation that exogenous dome growth results from fracturing along the conduit margin as ductile deformation of magma may no longer occur at high stresses.

Conclusions and Outlook

"I am careful not to confuse excellence with perfection. Excellence, I can reach for; perfection is God's business. "

M.J.Fox

Natural silicate melts exhibit complete and non linear behaviour and their rheology is time dependant. Concerning pure silicate liquids it has been largely demonstrated here that viscous heating is a first order phenomenon for the msot dynamics flows. Its onset is dependant of the stress and strain rate undergone by the system. Moreover its efficiency, linked to the Brinkman number, favours the re-distribution of the energy within the sample that may ease the brittle onset and lead to the cracks observed.

Viscous heating has also been observed in natural samples but at a much lower magnitude than in pure liquids. However the liquid fraction becomes lower with increasing crystal fraction. Consequently, the viscous heating could be of the same amplitude but localised within the liquid fraction and its effect may appear more diluted in the integrated volume.

Simple approximations support this idea. However, we will not speculate here, as the answer to this question may come with the future experiments (see below).

Concerning the effect of crystals on the rheology, we observed an instantaneous shear thinning effect followed by a time weakening effect. If the time weakening effect appears to be the consequence of crystals re-orientation and cracking, the instantaneous effect cause remains indeterminate. Here we propose an elastic effect as suggested by the loading-unloading tests. The uniaxial stress undergone by the crystal network may respond elastically and open channels for the melt to flow. Further tests will be conducted to confirm or invalidate this idea.

These results allow us to understand the strain-rate dependency of the apparent viscosity of natural silicate melts and its sources. It brings important outputs. Indeed, it shows that Einstein-Roscoe equation remains only valid for quasi-static processes. For higher strain-rates, the apparent viscosity can ultimately reach the viscosity of the interstitial melt and even lower if viscous heating is involved. The effect of crystals can be consequently completely cancelled.

This survey does not simply ends here. Many experience and collaborations are already engaged to answer the questions raised by our results. For example Brasil tests have already been performed to obtain the tensile strength of our sample and understand better the onset of the time weakening effect. The viscous heating effect is also planned to be extended to crystal be ring melts. Synthetics samples have been prepared in collaboration with the ETH Zürich. We hope to constrain the crystal fraction dependency of the viscous heating, if any. With the same sample set we expect to answer to the instantaneous effect issue.

Concerning pure liquids the remaining question concerns the brittle onset. It may find its answer while considering the energy stored by the sample. To do so, contacts have been already engaged with the University of Grenoble.

Finally our long term objectives are to develop a numerical simulation based on the level set method and able to treat multiphase flows with all the obser-

vations and results obtained above. This will offers a first time estimate of the apparent viscosity of natural melts for any stress and/or viscosity. It may also offer an evaluation of the acoustic energy released once the brittle onset is crossed. This will subsequently grant improved decisions and early warnings on active volcanic regions.

Bibliography

Allen, R. L. (1988), False pyroclastic textures in altered silicic lavas, with implications for volcanic-associated mineralization, *Economic Geology*, *83*(7), 1424–1446.

Allen, S. R., and J. McPhie (2003), Phenocryst fragments in rhyolitic lavas and lava domes, *Journal of Volcanology and Geothermal Research*, *126*(3-4), 263–283.

Avci, M., and O. Aydin (2008), Forced convection flow of viscous dissipative power-law fluids in a plane duct part 2. thermally developing flow, *Isi Bilimi Ve Teknigi Dergisi-Journal of Thermal Science and Technology*, *28*(2), 17–24.

Bagdassarov, N. S., D. B. Dingwell, and S. L. Webb (1994), Viscoelasticity of crystal-bearing and bubble-bearing rhyolite melts, *Physics of the Earth and Planetary Interiors*, *83*(2), 83–99.

Bagnold, R. (1954), Experiments on a gravity-free dispersion of large solid spheres in a newtonian fluid under shear., *Proc. R. Soc. London, Ser. A225*, 49–63.

Batchelor, G. K. (1977), Effect of brownian-motion on bulk stress in a suspension of spherical-particles, *Journal of Fluid Mechanics*, *83*(NOV), 97–117.

Batchelor, G. K., and J. T. Green (1972), Determination of bulk stress in a suspension of spherical-particles to order c-2, *Journal of Fluid Mechanics*, *56*(DEC12), 401–427.

Becker, L. E., and G. H. Mkinley (2000), The stability of viscoelastic creeping plane shear flows with viscous heating, *Journal of Non-Newtonian Fluid Mechanics*, *92*(2-3), 109–133.

Bercovici, D. (1998), Generation of plate tectonics from lithosphere-mantle flow and void-volatile self-lubrication, *Earth and Planetary Science Letters*, *154*(1-4), 139–151.

Best, M. G., and E. H. Christiansen (1997), Origin of broken phenocrysts in ash-flow tuffs, *Geological Society of America Bulletin*, *109*(1), 63–73.

Booth, B., and S. Self (1973), Rheological features of 1971 mount etna lavas, *Philosophical Transactions of the Royal Society of London Series a-Mathematical Physical and Engineering Sciences*, *274*(1238), 99–106.

Bowden, P. B. (1970), A criterion for inhomogeneous plastic deformation, *Philosophical Magazine*, *22*(177), 455–462.

Bowden, P. B., and J. A. Jukes (1969), Deformation bands in amorphous polystyrene and their relation to slip line field, *Nature*, *221*(5179), 462–463.

Boyd, F. (1961), Welded tuffs and flows in the rhyolite plateau of yellowstone park, wyoming, *Bull. Geol. Soc. Am.*, p. 387426.

Braeck, S., and Y. Y. Podladchikov (2007), Spontaneous thermal runaway as an ultimate failure mechanism of materials, *Physical Review Letters*, *98*(9), 4.

Branney, M. J., B. P. Kokelaar, and B. J. McConnell (1992), The bad step tuff - a lava-like rheomorphic ignimbrite in a calc-alkaline piecemeal caldera, english lake district, *Bulletin of Volcanology*, *54*(3), 187–199.

Brinkman, H. C. (1950), Heat effects in capillary flow-i, *Applied Scientific Research Section a-Mechanics Heat Chemical Engineering Mathematical Methods*, *2*(2), 120–124.

Bruckner, R., and J. Deubener (1997), Description and interpretation of the two phase flow behaviour of melts with suspended crystals, *Journal of Non-Crystalline Solids*, *209*(3), 283–291.

Brun, J. P., and P. R. Cobbold (1980), Strain heating and thermal softening in continental shear zones - a review, *Journal of Structural Geology*, *2*(1-2), 149–158.

Burg, J. P., and T. V. Gerya (2005), The role of viscous heating in barrovian metamorphism of collisional orogens: thermomechanical models and application to the lepontine dome in the central alps, *Journal of Metamorphic Geology*, *23*(2), 75–95.

Burg, J. P., and S. M. Schmalholz (2008), Viscous heating allows thrusting to overcome crustal-scale buckling: Numerical investigation with application to the himalayan syntaxes, *Earth and Planetary Science Letters*, *274*(1-2), 189–203.

Calado, V. M. A., J. M. White, and S. J. Muller (2005), Transient behavior of boger fluids under extended shear flow in a cone-and-plate rheometer, *Rheologica Acta*, *44*(3), 250–261.

Canova, G., C. Gsell, and J. J. Jonas (1980), Localization of tensile plastic-flow in material insensitive to rate of deformation, *Canadian Metallurgical Quarterly*, *19*(2), 259–263.

Caricchi, L., L. Burlini, P. Ulmer, T. Gerya, M. Vassalli, and P. Papale (2007), Non-newtonian rheology of crystal-bearing magmas and implications for magma ascent dynamics, *Earth and Planetary Science Letters*, *264*(3-4), 402–419.

Carrigan, C. R., G. Schubert, and J. C. Eichelberger (1992), Thermal and dynamic regimes of single-phase and 2-phase magmatic flow in dikes, *Journal of Geophysical Research-Solid Earth*, *97*(B12), 17,377–17,392.

Champallier, R., M. Bystricky, and L. Arbaret (2008), Experimental investigation of magma rheology at 300 mpa: From pure hydrous melt to 76 vol.percent of crystals, *Earth and Planetary Science Letters*, *267*(3-4), 571–583.

Chong, J., E. Christiansen, and A. Baer (1971), Rheology of concentrated suspensions., *J. Appl. Polym. Sci.*, *15*, 2007–2021.

Coelho, P., and F. Pinhoa (2009), A generalized brinkman number for non-newtonian duct flows, *J. Non-Newtonian Fluid Mech.*, *156*, 202206.

Costa, A. (2005), Viscosity of high crystal content melts: Dependence on solid fraction, *Geophysical Research Letters*, *32*(22), L22,308.

Costa, A., and G. Macedonio (2003a), Viscous heating in fluids with temperature-dependent viscosity: implications for magma flows, *Nonlinear Processes in Geophysics*, *10*(6), 545–555.

Costa, A., and G. Macedonio (2003b), Viscous heating in fluids with temperature-dependent viscosity: implications for magma flows, *Nonlinear Processes in Geophysics*, *10*(6), 545–555.

Costa, A., and G. Macedonio (2005), Viscous heating effects in fluids with temperature-dependent viscosity: triggering of secondary flows, *Journal of Fluid Mechanics*, *540*, 21–38.

Costa, A., O. Melnik, and R. S. J. Sparks (2007), Controls of conduit geometry and wallrock elasticity on lava dome eruptions, *Earth and Planetary Science Letters*, *260*(1-2), 137–151.

Deubener, J., and R. Bruckner (1997), Influence of nucleation and crystallisation on the rheological properties of lithium disilicate melt, *Journal of Non-Crystalline Solids*, *209*(1-2), 96–111.

Dingwell, D. B. (1996), Volcanic dilemma–flow or blow?, *Science*, *273*(5278), 1054–1055.

Dingwell, D. B., and S. L. Webb (1989), Structural relaxation in silicate melts and non-newtonian melt rheology in geologic processes, *Physics and Chemistry of Minerals*, *16*(5), 508–516.

Dingwell, D. B., and S. L. Webb (1990), Relaxation in silicate melts., *European Journal of Mineralogy*, *2*, 427–449.

Dingwell, D. B., K. U. Hess, and C. Romano (1998), Viscosity data for hydrous peraluminous granitic melts: Comparison with a metaluminous model., *American Mineralogist*, *83*(3-4), 236–239.

D'Oriano, C., E. Poggianti, A. Bertagnini, R. Cioni, P. Landi, M. Polacci, and M. Rosi (2005), Changes in eruptive style during the ad 1538 monte nuovo eruption (phlegrean fields, italy): the role of syn-eruptive crystallization, *Bulletin of Volcanology*, *67*(7), 601–621.

Dragoni, M., F. D'Onza, and A. Tallarico (2002), Temperature distribution inside and around a lava tube, *Journal of Volcanology and Geothermal Research*, *115*(1-2), 43–51.

Eilers, H. (1941), Die viskositt von emulsionen hochviskoser stoffe als funktion der konzentration, *Colloid & Polymer Science*, *97*(3), 313–321.

Fisher, R., and H. Schmincke (1984), *Pyroclastic Rocks*, Springer-Verlag, New York.

Frost, H. J., and M. F. Ashby (Eds.) (1982), *Deformation-Mechanism Maps: The Plasticity and Creep of Metals and Ceramics.*, 1st ed edition ed., Pergamon Press.

Fujii, N., and S. Uyeda (1974), Thermal instabilities during flow of magma in volcanic conduits, *Journal of Geophysical Research*, *79*(23), 3367–3369.

Fujii, T., and S. Nakada (1999), The 15 september 1991 pyroclastic flows at unzen volcano (japan): a flow model for associated ash-cloud surges, *Journal of Volcanology and Geothermal Research*, *89*(1-4), 159–172.

Fujita, E., Y. Fukao, and K. Kanjo (2000), Strain offsets with monotonous damped oscillations during the 1986 izu-oshima volcano eruption, *Journal of Geophysical Research-Solid Earth*, *105*(B1), 443–462.

Fukui, K., T. Hashimoto, K. Uhira, H. Yamasato, T. Koizumi, H. Mori, Y. Ueda, and J. Akiyoshi (1991), Growth and movement of the unzendake lava dome, in *The fall Meeting of the Volcanological Society of Japan, 38.*

Gadalamaria, F., and A. Acrivos (1980), Shear-induced structure in a concentrated suspension of solid spheres, *Journal of Rheology, 24*(6), 799–814.

Gallop, P. M. (1955), Particle size and shape in a citrate extract of ichthyocol, *Archives of Biochemistry and Biophysics, 54*(2), 486–500.

Garrigues, J. (2007), *Fondements de la mcanique des milieux continus*, 250 p. pp.

Gay, E. C., P. A. Nelson, and W. P. Armstrong (1969), Flow properties of suspensions with high solids concentration, *AICHe Journal, 15*(6), 815–822.

Gent, A. N. (1960), Theory of the parallel plate viscometer, *British Journal of Applied Physics, 11*(2), 85–87.

Gerya, T. V., and D. A. Yuen (2003), Rayleigh-taylor instabilities from hydration and melting propel 'cold plumes' at subduction zones, *Earth and Planetary Science Letters, 212*(1-2), 47–62.

Gonnermann, H. M., and M. Manga (2003), Explosive volcanism may not be an inevitable consequence of magma fragmentation, *Nature, 426*(6965), 432–435.

Gonnermann, H. M., and M. Manga (2005), Flow banding in obsidian: A record of evolving textural heterogeneity during magma deformation, *Earth and Planetary Science Letters, 236*(1-2), 135–147.

Gonnermann, H. M., and M. Manga (2007), The fluid mechanics inside a volcano, *Annual Review of Fluid Mechanics, 39*, 321–356.

Goto, A. (1999), A new model for volcanic earthquake at unzen volcano: Melt rupture model, *Geophysical Research Letters*, *26*(16), 2541–2544.

Gottsmann, J., and D. Dingwell (2000), Supercooled diopside melt: confirmation of temperature-dependent expansivity using container-based dilatometry, *Contributions to Mineralogy and Petrology*, *139*(2), 127–135.

Greeley, R., S. A. Fagents, R. S. Harris, S. D. Kadel, D. A. Williams, and J. E. Guest (1998), Erosion by flowing lava: Field evidence, *Journal of Geophysical Research-Solid Earth*, *103*(B11), 27,325–27,345.

Griggs, D. T., F. J. Turner, and H. C. Heard (1960), Deformation of rocks at 500 to 800., in *Rock Deformation - A Symposium*, vol. 79, edited by D. Griggs and J. Handin, p. 39104, Geol. Soc. Amer. Memoir.

Hale, A. J., and H.-B. Muhlhaus (2007), Modelling shear bands in a volcanic conduit: Implications for over-pressures and extrusion-rates, *Earth and Planetary Science Letters*, *263*(1-2), 74–87.

Hardee, H. C., and D. W. Larson (1977), Viscous dissipation effects in magma conduits, *Journal of Volcanology and Geothermal Research*, *2*(3), 299–308.

Hartz, E. H., and Y. Y. Podladchikov (2008), Toasting the jelly sandwich: The effect of shear heating on lithospheric geotherms and strength, *Geology*, *36*(4), 331–334.

Hawkes, I., and M. Mellor (1970), Uniaxial testing in rock mechanics laboratories, *Engineering Geology*, *4*(3), 177–285.

Hess, K. U., and D. B. Dingwell (1996), Viscosities of hydrous leucogranitic melts: A non-arrhenian model, *American Mineralogist*, *81*(9-10), 1297–1300.

Hess, K. U., D. B. Dingwell, and S. L. Webb (1995), The influence of excess alkalis on the viscosity of a haplogranitic melt, *American Mineralogist*, *80*(3-4), 297–304.

Hess, K. U., D. B. Dingwell, C. Gennaro, and V. Mincione (2001), Viscosity-temperature behaviour of dry melts in the qz-ab-or system, *Chemical Geology*, *174*(1-3), 133–142.

Hess, K. U., B. Cordonnier, Y. Lavallee, and D. B. Dingwell (2007), High-load, high-temperature deformation apparatus for synthetic and natural silicate melts, *Review of Scientific Instruments*, *78*(7), 075,102–075,106.

Hess, K. U., B. Cordonnier, Y. Lavallee, and D. B. Dingwell (2008), Viscous heating in rhyolite: An in situ experimental determination, *Earth and Planetary Science Letters*, *275*(1-2), 121–126.

Holtz, F., H. Sato, J. Lewis, H. Behrens, and S. Nakada (2005), Experimental petrology of the 1991-1995 unzen dacite, japan. part i: Phase relations, phase composition and pre-eruptive conditions, *Journal of Petrology*, *46*(2), 319–337.

Holtzman, B. K., D. L. Kohlstedt, and J. P. Morgan (2005), Viscous energy dissipation and strain partitioning in partially molten rocks, *Journal of Petrology*, *46*(12), 2569–2592.

Jaworski, B., and A. Detlaf (1972), *Physik griffbereit. Definitionen - Gesetze - Theorien*, Berlin: Akademie Verlag.

Jeffrey, D. J., and A. Acrivos (1976), Rheological properties of suspensions of rigid particles, *Aiche Journal*, *22*(3), 417–432.

Jonas, J. J., R. A. Holt, and C. E. Coleman (1976), Plastic stability in tension and compression, *Acta Metallurgica*, *24*(10), 911–918.

Jones, D., B. Leary, and D. V. Boger (1991), The rheology of a concentrated colloidal suspension of hard spheres., *Journal of Colloid and Interface Science*, *147*, 479–495.

Jones, D., B. Leary, and D. V. Boger (1992), The rheology of a sterically stabilized suspension at high concentration., *Journal of Colloid and Interface Science*, *150*, 84–96.

Kameyama, M., and Y. Kaneda (2002), Thermal-mechanical coupling in shear deformation of viscoelastic material as a model of frictional constitutive relations, *Pure and Applied Geophysics*, *159*(9), 2011–2028.

Kameyama, M., D. A. Yuen, and H. Fujimoto (1997), The interaction of viscous heating with grain-size dependent rheology in the formation of localized slip zones, *Geophysical Research Letters*, *24*(20), 2523–2526.

Kameyama, M., D. A. Yuen, and S. I. Karato (1999), Thermal-mechanical effects of low-temperature plasticity (the peierls mechanism) on the deformation of a viscoelastic shear zone, *Earth and Planetary Science Letters*, *168*(1-2), 159–172.

Karato, S. I., M. S. Paterson, and J. D. Fitz Gerald (1986), Rheology of synthetic olivine aggregates - influence of grain-size and water, *Journal of Geophysical Research-Solid Earth and Planets*, *91*(B8), 8151–8176.

Kato, H., A. Inoue, and H. S. Chen (2003), Heating and structural disordering effects of the nonlinear viscous flow in a zr55al10ni5cu30 bulk metallic glass, *Applied Physics Letters*, *83*(26), 5401–5403.

Kato, H., A. Inoue, and H. S. Chen (2006), On structural relaxation and viscous work heating during non-newtonian viscous flow in a zr55al10ni5cu30 bulk metallic glass, *Acta Materialia*, *54*(4), 891–898.

Kato, H., A. Inoue, and H. S. Chen (2007), Softening and heating behaviors during the nonlinear viscous flow in a zr-based bulk metallic glass, *Journal of Non-Crystalline Solids*, *35*, 3764–3768.

Kaus, B. J. P., and Y. Y. Podladchikov (2006), Initiation of localized shear zones in viscoelastoplastic rocks, *Journal of Geophysical Research-Solid Earth*, *111*(B4).

Kearsley, E. A. (1962), The viscous heating correction for viscometer flows, *Transactions of the Society of Rheology*, *6*, 253–261.

Kennedy, B., O. Spieler, B. Scheu, U. Kueppers, J. Taddeucci, and D. B. Dingwell (2005), Conduit implosion during vulcanian eruptions, *Geology*, *33*(7), 581–584.

Keszthelyi, L. (1995a), A preliminary thermal budget for lava tubes on the earth and planets, *Journal of Geophysical Research-Solid Earth*, *100*(B10), 20,411–20,420.

Keszthelyi, L. (1995b), Measurements of the cooling at the base of pahoehoe flows, *Geophysical Research Letters*, *22*(16), 2195–2198.

Keszthelyi, L. (1995c), A preliminary thermal budget for lava tubes on the earth and planets, *Journal of Geophysical Research-Solid Earth*, *100*(B10), 20,411–20,420.

Knoche, R., D. B. Dingwell, and S. L. Webb (1995), Melt densities for leukogranites and granitic pegmatites - partial molar volumes for sio2, al2o3, na2o, k2o, li2o, rb2o, cs2o, mgo, cao, sro, bao, b2o3, p2o5, f2o-1, tio2, nb2o5, ta2o5, and wo3, *Geochimica Et Cosmochimica Acta*, *59*(22), 4645–4652.

Krieger, I. M., and T. J. Dougherty (1959), A mechanism for non-newtonian flow in suspensions of rigid spheres, *Transactions of the Society of Rheology*, *3*, 137–152.

Kueppers, U., B. Scheu, O. Spieler, and D. B. Dingwell (2006), Fragmentation efficiency of explosive volcanic eruptions: A study of experimentally generated pyroclasts, *Journal of Volcanology and Geothermal Research*, *153*(1-2), 125–135.

Kusakabe, M., H. Sato, S. Nakada, and T. Kitamura (1999), Water contents and hydrogen isotopic ratios of rocks and minerals from the 1991 eruption of unzen volcano, japan, *Journal of Volcanology and Geothermal Research*, *89*(1-4), 231–242.

Larsen, T. B., D. A. Yuen, and A. V. Malevsky (1995), Dynamical consequences on fast subducting slabs from a self-regulating mechanism due to viscous heating in variable viscosity convection, *Geophysical Research Letters*, *22*(10), 1277–1280.

Lavallee, Y., K. U. Hess, B. Cordonnier, and D. Dingwell (2007), Non-newtonian rheological law for highly crystalline dome lavas, *Geology*, *35*(9), 843–846.

Lavallee, Y., P. G. Meredith, D. B. Dingwell, K. U. Hess, J. Wassermann, B. Cordonnier, A. Gerik, and J. H. Kruhl (2008), Seismogenic lavas and explosive eruption forecasting, *Nature*, *453*(7194), 507–510.

Lejeune, A. M., and P. Richet (1995), Rheology of crystal-bearing silicate melts - an experimental-study at high viscosities, *Journal of Geophysical Research-Solid Earth*, *100*(B3), 4215–4229.

Maeda, I. (2000), Nonlinear visco-elastic volcanic model and its application to the recent eruption of mt. unzen, *Journal of Volcanology and Geothermal Research*, *95*(1-4), 35–47.

Massol, H., and C. Jaupart (1999), The generation of gas overpressure in volcanic eruptions, *Earth and Planetary Science Letters*, *166*(1-2), 57–70.

Massol, H., and T. Koyaguchi (2005), The effect of magma flow on nucleation of gas bubbles in a volcanic conduit, *Journal of Volcanology and Geothermal Research*, *143*(1-3), 69–88.

Massol, H., C. Jaupart, and D. W. Pepper (2001), Ascent and decompression of viscous vesicular magma in a volcanic conduit, *Journal of Geophysical Research-Solid Earth*, *106*(B8), 16,223–16,240.

Mastin, L. G. (2002), Insights into volcanic conduit flow from an open-source numerical model, *Geochemistry Geophysics Geosystems*, *3*.

Mastin, L. G. (2005a), The controlling effect of viscous dissipation on magma flow in silicic conduits, *Journal of Volcanology and Geothermal Research*, *143*(1-3), 17–28.

Mastin, L. G. (2005b), The controlling effect of viscous dissipation on magma flow in silicic conduits, *Journal of Volcanology and Geothermal Research*, *143*, 17–28.

Maxwell, J. (1866), On the dynamical theory of gases, *Philosophical Transactions of the Royal Society of London*, *157*, 49–88.

Melnik, O., and R. S. J. Sparks (1999), Nonlinear dynamics of lava dome extrusion, *Nature*, *402*(6757), 37–41.

Melnik, O., A. A. Barmin, and R. S. J. Sparks (2005), Dynamics of magma flow inside volcanic conduits with bubble overpressure buildup and gas loss through permeable magma, *Journal of Volcanology and Geothermal Research*, *143*(1-3), 53–68.

Mooney, M. (1951), The viscosity of a concentrated suspension of spherical particles, *Journal of Colloid Science*, *6*(2), 162–170.

Murrell, S. A. F., and S. Chakravarty (1973), Some new rheological experiments on igneous rocks at temperatures up to 1120 degrees c, *Geophysical Journal of the Royal Astronomical Society*, *34*(2), 211–250.

Mysen, B. (1987), Magmatic silicate melts: relations between bulk composition, structure and properties. in: B.o. mysen, editor, magmatic processes: Physicochemical principles, *Geochemical Society Special Publication*, p. 375400.

Nakada, S., and Y. Motomura (1999), Petrology of the 1991-1995 eruption at unzen: effusion pulsation and groundmass crystallization, *Journal of Volcanology and Geothermal Research*, *89*(1-4), 173–196.

Nakada, S., H. Shimizu, and K. Ohta (1999), Overview of the 1990-1995 eruption at unzen volcano, *Journal of Volcanology and Geothermal Research*, *89*(1-4), 1–22.

Neuberg, J. W., H. Tuffen, L. Collier, D. Green, T. Powell, and D. Dingwell (2006), The trigger mechanism of low-frequency earthquakes on montserrat, *Journal of Volcanology and Geothermal Research*, *153*(1-2), 37–50.

Nicolas, A. (1984), *Principes de tectonique*, Masson.

Nicolas, A., J. L. Bouchez, J. Blaise, and J. P. Poirier (1977), Geological aspects of deformation in continental shear zones, *Tectonophysics*, *42*(1), 55–73.

Nishiyama, N., and A. Inoue (1999), Glass transition behavior and viscous flow working of pd40cu30ni10p20 amorphous alloy, *Materials Transactions Jim*, *40*(1), 64–71.

Noguchi, S., A. Toramaru, and S. Nakada (2007), Groundmass crystallization process in the dacite dikes of unzen scientific drilling project 4 (usdp4), in *Cities On Volcanoes 5*.

Noguchi, S., A. Toramaru, and S. Nakada (2008), Groundmass crystallization in dacite dykes taken in unzen next term scientific drilling project (usdp-4), *Journal of Volcanology and Geothermal Research*, *175*, 71–81.

Ostwald, W. (1925), Ueber die geschwindigkeitsfunktion der viskositt disperser systeme. i, *Colloid and Polymer Science*, *36*(2), 99–117.

Papathanasiou, T., K. Caridis, and B. Bijeljic (1997), Thermomechanical coupling in frictionally heated circular couette flow, *International Journal of Thermophysics*, *18*(3), 825–843.

Paterson, M. S. (1958), Experimental deformation and faulting in wombeyan marble, *Geological Society of America Bulletin*, *69*(4), 465–475.

Pearson, J. R. A. (1977), Variable-viscosity flows in channels with high heat-generation, *Journal of Fluid Mechanics*, *83*(NOV), 191–206.

Platt, J. P., and P. C. England (1994), Convective removal of lithosphere beneath mountain belts - thermal and mechanical consequences, *American Journal of Science*, *294*(3), 307–336.

Poirier, J. P. (1980), Shear localization and shear instability in materials in the ductile field, *Journal of Structural Geology*, *2*(1-2), 135–142.

Poirier, J. P. (1985), *Creep of crystals: high-temperature deformation processes in metals, ceramics and minerals*, Cambridge (Cambridge University Press; Earth Science Series).

Poirier, J. P., J. L. Bouchez, and J. J. Jonas (1979), Dynamic-model for aseismic ductile shear zones, *Earth and Planetary Science Letters*, *43*(3), 441–453.

Polacci, M. (2005), Constraining the dynamics of volcanic eruptions by characterization of pumice textures, *Annals of Geophysics*, *48*(4-5), 731–738.

Polacci, M., P. Papale, and M. Rosi (2001), Textural heterogeneities in pumices from the climactic eruption of mount pinatubo, 15 june 1991, and implications for magma ascent dynamics, *Bulletin of Volcanology*, *63*(2-3), 83–97.

Polacci, M., P. Papale, D. Del Seppia, D. Giordano, and C. Romano (2004), Dynamics of magma ascent and fragmentation in trachytic versus rhyolitic eruptions, *J. Volcanol. Geotherm. Res.*, *131*(12), 93108.

Potuzak, M., and D. B. Dingwell (2006), Temperature-dependent thennal. expansivities of multicomponent natural melts between 993 and 1803 k, *CHEMICAL GEOLOGY*, *229*, 10–27.

Reiner, M. (1964), The deborah number, *Physic Today*, *1*, 62.

Romano, C., J. E. Mungall, T. Sharp, and D. B. Dingwell (1996), Tensile strengths of hydrous vesicular glasses: An experimental study, *American Mineralogist*, *81*(9-10), 1148–1154.

Roscoe, R. (1952), The viscosity of suspensions of rigid spheres, *British Journal of Applied Physics*, *3*(AUG), 267–269.

Rosi, M., P. Landi, M. Polacci, A. Di Muro, and D. Zandomeneghi (2004), Role of conduit shear on ascent of the crystal-rich magma feeding the 800-year-bp plinian eruption of quilotoa volcano (ecuador), *Bulletin of Volcanology*, *66*(4), 307–321.

Rummel, F., and C. Fairhurst (1970), Determination of the post-failure behavior of brittle rock using a servo-controlled testing machine, *Rock Mechanics and Rock Engineering*, *2*(4), 189–204.

Rutter, E. H., and D. H. K. Neumann (1995), Experimental deformation of partially molten westerly granite under fluid-absent conditions, with implications for the extraction of granitic magmas, *Journal of Geophysical Research-Solid Earth*, *100*(B8), 15,697–15,715.

Ryerson, F. J., H. C. Weed, and A. J. Piwinskii (1988), Rheology of subliquidus magmas .1. picritic compositions, *Journal of Geophysical Research-Solid Earth and Planets*, *93*(B4), 3421–3436.

Schott, B., D. A. Yuen, and H. Schmeling (1999), Viscous heating in heterogeneous media as applied to the thermal interaction between the crust and mantle, *Geophysical Research Letters*, *26*(4), 513–516.

Schubert, G., and D. A. Yuen (1978), Shear heating instability in earths upper mantle, *Tectonophysics*, *50*(2-3), 197–205.

Shaw, H. R. (1969), Rheology of basalt in melting range, *Journal of Petrology*, *10*(3), 510–&.

Shea, W., and A. K. Kronenberg (1992), Rheology and deformation mechanisms of an isotropic mica shist., *Journal of Geophysical Research*, *97*, 15,201–15,237.

Simmons, J., R. Mohr, and C. Montrose (1982a), Viscous failure of glass at high shear rates, *J. Phys.*, *43*(NC-9), 439442.

Simmons, J. H., R. K. Mohr, and C. J. Montrose (1982b), Non-newtonian viscous-flow in glass, *Journal of Applied Physics*, *53*(6), 4075–4080.

Simmons, J. H., R. Ochoa, K. D. Simmons, and J. J. Mills (1988), Non-newtonian viscous-flow in soda-lime silica glass at forming and annealing temperatures, *Journal of Non-Crystalline Solids*, *105*(3), 313–322.

Smellie, J. L., I. L. Millar, D. C. Rex, and P. J. Butterworth (1998), Subaqueous, basaltic lava dome and carapace breccia on king george island, south shetland islands, antarctica, *Bulletin of Volcanology*, *59*(4), 245–261.

Sparks, R. S. J., M. D. Murphy, A. M. Lejeune, R. B. Watts, J. Barclay, and S. R. Young (2000), Control on the emplacement of the andesite lava dome of the soufriere hills volcano, montserrat by degassing-induced crystallization, *Terra Nova*, *12*(1), 14–20.

Spieler, O., B. Kennedy, U. Kueppers, D. B. Dingwell, B. Scheu, and J. Taddeucci (2004), The fragmentation threshold of pyroclastic rocks, *Earth and Planetary Science Letters*, *226*(1-2), 139–148.

Stein, D., and F. Spera (1992), Rheology and microstructure of magmatic emulsionstheory and experiments, *J. Volcanol. Geotherm. Res.*, *49*(12), 157174.

Strivens, T. A. (1983), The viscoelastic properties of concentrated suspensions, *Colloid and Polymer Science*, *261*(1), 74–81.

Suto, S., K. Sakaguchi, K. Watanabe, E. Saito, Y. Kawanabe, K. Kazahaya, S. Takarada, and T. Soya (1993), Dynamics of flowage and viscosity of the 1991 lava of unzen volcano,kyushu, japan, *Bull. Geol. Surv. Japan*, *44*, 609–629.

Thomas, D. G. (1965), Transport characteristics of suspension: Viii. a note on the viscosity of newtonian suspensions of uniform spherical particles, *Journal of Colloid Science.*, *20*(3), 267–277.

Tuffen, H., and D. Dingwell (2005), Fault textures in volcanic conduits: evidence for seismic trigger mechanisms during silicic eruptions, *Bulletin of Volcanology*, *67*(4), 370–387.

Tuffen, H., D. B. Dingwell, and H. Pinkerton (2003), Repeated fracture and healing of silicic magma generate flow banding and earthquakes?, *Geology*, *31*(12), 1089–1092.

Tuffen, H., R. Smith, and P. R. Sammonds (2008), Evidence for seismogenic fracture of silicic magma, *Nature*, *453*(7194), 511–514.

Turian, R. M. (1965), Viscous heating in cone-and-plate viscometer .3. non-newtonian fluids with temperature-dependent viscosity and thermal conductivity, *Chemical Engineering Science*, *20*(8), 771–&.

Turian, R. M., and R. B. Bird (1963), Viscous heating in the cone-and-plate viscometer .2. newtonian fluids with temperature-dependent viscosity and thermal conductivity, *Chemical Engineering Science*, *18*(11), 689–696.

Vand, V. (1948), Viscosity of solutions and suspensions. ii. experimental determination of the viscosity-concentration function of spherical suspensions., *J. Phys. Coll. Chem.*, *52*, 300–314.

Vandermolen, I., and M. S. Paterson (1979), Experimental deformation of partially-melted granite, *Contributions to Mineralogy and Petrology*, *70*(3), 299–318.

Vedeneeva, E. A., O. E. Melnik, A. A. Barmin, and R. S. J. Sparks (2005), Viscous dissipation in explosive volcanic flows, *Geophysical Research Letters*, *32*(5).

Voight, B., et al. (1999), Magma flow instability and cyclic activity at soufriere hills volcano, montserrat, british west indies, *Science*, *283*(5405), 1138–1142.

Ward, S. G., and R. L. Whitmore (1950a), Studies of the viscosity and sedimentation of suspensions, part 1.-the viscosity of suspension of spherical particles., *British Journal of Applied Physics*, *1*, 286–290.

Ward, S. G., and R. L. Whitmore (1950b), Studies of the viscosity and sedimentation of suspensions, part 2.-the viscosity and sedimentation of suspension of rough powders., *British Journal of Applied Physics*, *1*, 325–328.

Webb, S. L., and D. B. Dingwell (1990a), Non-newtonian rheology of igneous melts at high stresses and strain rates - experimental results for rhyolite, andesite, basalt, and nephelinite, *Journal of Geophysical Research-Solid Earth and Planets*, *95*(B10), 15,695–15,701.

Webb, S. L., and D. B. Dingwell (1990b), The onset of non-newtonian rheology of silicate melts - a fiber elongation study, *Physics and Chemistry of Minerals*, *17*(2), 125–132.

Webb, S. L., and D. B. Dingwell (1995), Viscoelasticity, in *Structure, Dynamics and Properties of Silicate Melts*, *Reviews in Mineralogy*, vol. 32, pp. 95–119, Mineralogical Soc America, Washington.

White, J. M., and S. J. Muller (2000a), Viscous heating and the stability of newtonian and viscoelastic taylor-couette flows, *Physical Review Letters*, *84*(22), 5130–5133.

White, J. M., and S. J. Muller (2000b), Viscous heating and the stability of newtonian and viscoelastic taylor-couette flows, *Physical Review Letters*, *84*(22), 5130–5133.

White, J. M., and S. J. Muller (2002a), Experimental studies on the stability of newtonian taylor-couette flow in the presence of viscous heating, *Journal of Fluid Mechanics*, *462*, 133–159.

White, J. M., and S. J. Muller (2002b), The role of thermal sensitivity of fluid properties, centrifugal destabilization, and nonlinear disturbances on the viscous heating instability in newtonian taylor-couette flow, *Physics of Fluids*, *14*(11), 3880–3890.

Woutersen, A., and C. Kruif (1991), The rheology of adhesive hard sphere dispersions., *J. Chem. Phys.*, *94*, 5739–5750.

Yue, Y., and R. Brckner (1994), A new description and interpretation of the flow behaviour of glass forming melts, *Journal of Non-Crystalline Solids*, *180*(1), 66–79.

Benoît Cordonnier

Education

Present Day – August 2005
PhilosophiæDoctor work at the Ludwig Maximilians Universität.
"Non-Newtonian effects in silicate liquids and crystal bearing melts: Implication for magma dynamics", München (Germany). Fieldwork: Teneriffe (Canary Islands)

October 2004
DEA Geoscienses with merit at the University of Rennes 1.
Professional training of research for 7 months:"Kinematic and internal deformation in lava flows by analogs material", University of the Reunion St. Denis (Island of the Reunion).

June 2003
Maitrise of Earth's Sciences with merit at the University of Rennes 1.
Training course of research for 3 months:"Adequacy of Numeric digital code THEMA to lava flows". Commissariat à l'Energie Atomique (French Atomic Center), Cadarache (France). T.E.R. (Work of study and research): "Application of the imbalances radioactives chains to the volcanic systems". Field work: April, structural study of the Dévoluy and Chaillol's massif (French Alps); October, Geomorphological study of the central Pyrenées

June 2002
License of Earth's Sciences (Bsc) at the University of Rennes 1.
Field work: April, cartography in the eastern Pyrenées; October, "Transbreizh", structural petrologic and sedimentary study of the Armorican southern massif

June 2001
DEUG of matter sciences (Physics).
Field work: October, structural,petrologic and sedimentary study of the Pyrenées

June 1999
College Preparatory School of the "Beaux Arts". National French Art School.

Experience

October 2008 – May 2008
Employee for a regional newspaper, *Ouest France*, Rennes (France).

Summer 2003
Second of Kitchen, Sauzon, Belle île en Mer.

Summer 2002
Assistant of Kitchen, Sauzon, Belle île en Mer.

2001 – 2002
Specific missions as Security Agent, *Agence Bretonne de Sécurité*, Rennes (France).

Summer 2001 – Summer 2000
Sales person, *Select Disc Organisation compagny*, Domloup (France).

Winter 2000 – Summer 1999
Alternatively Barman & Host of case, Rennes- Châteaugiron (France).

Languages

French	Mother tongue
English	Fluent
Spanish	Intermediate
German	Basic

☎ +49 089-2180 4271 • ✉ cordonnier@min.uni-muenchen.de

Computer skills

Software	Illustrator, Photoshop, 3Ds Max, FREEFEM, Comsol	Languages	C, FORTRAN, Matlab
Op. Sytem	Windows, Linux & MacOs X Windows & Linux administration skills,	Bureautic	Open & Microsoft office, LaTeX

Publications

2009 *Cordonnier, B., S. M. Schmalholz, et al. "Viscous Heating, Non-Newtonian and Brittle onset: An energy interaction." Earth and Planetary Science Letters SUBMITTED*

2009 *Cordonnier, B., K. U. Hess, et al. "Rheological properties of dome lavas: Case study of Unzen volcano." Earth and Planetary Science Letters In Press, Corrected Proof.*

2008 *Lavallee, Y., P. G. Meredith, et al. "Seismogenic lavas and explosive eruption forecasting." Nature 453(7194): 507-510.*

2008 *Hess, K. U., B. Cordonnier, et al. (2008). "Viscous heating in rhyolite: An in situ experimental determination." Earth and Planetary Science Letters 275(1-2): 121-126.*

2007 *Lavallee, Y., K. U. Hess, et al. (2007). "Non-Newtonian rheological law for highly crystalline dome lavas." Geology 35(9): 843-846.*

2007 *Hess, K. U., B. Cordonnier, et al. (2007). "High-load, high-temperature deformation apparatus for synthetic and natural silicate melts." Review of Scientific Instruments 78(7): 075102-4.*

Interests

Sports	Judo (Gr: Black Belt, Ex-member of the Dojo Casltegironnais council, Member of the national black belt college)	Others	Surf, Snow-Board, Tennis, Cannoyning
Intellectual interests	Astrophysic (Ex-Member of the "Société Astronomique de Rennes), Volcanlogy,Drawing, Opera, Photography	Others	Geopolitic, Humanitarian help